AMERICAN SOCIETY FOR MICROBIOLOGY | Journal of Virology®

PATHOGENESIS AND IMMUNITY

Attenuation of Influenza A Virus Disease Severity by Viral Coinfection in a Mouse Model

Andres J. Gonzalez,[a] Emmanuel C. Ijezie,[a] Onesmo B. Balemba,[a,b] Tanya A. Miura[a]

[a]Department of Biological Sciences and Center for Modeling Complex Interactions, University of Idaho, Moscow, Idaho, USA

[b]Idaho WWAMI Medical Education Program, University of Idaho, Moscow, Idaho, USA

ABSTRACT Influenza viruses and rhinoviruses are responsible for a large number of acute respiratory viral infections in human populations and are detected as copathogens within hosts. Clinical and epidemiological studies suggest that coinfection by rhinovirus and influenza virus may reduce disease severity and that they may also interfere with each other's spread within a host population. To determine how coinfection by these two unrelated respiratory viruses affects pathogenesis, we established a mouse model using a minor serogroup rhinovirus (rhinovirus strain 1B [RV1B]) and mouse-adapted influenza A virus (A/Puerto Rico/8/1934 [PR8]). Infection of mice with RV1B 2 days before PR8 reduced the severity of infection by a low or medium, but not high, dose of PR8. Disease attenuation was associated with an early inflammatory response in the lungs and enhanced clearance of PR8. However, coinfection by RV1B did not reduce PR8 viral loads early in infection or inhibit replication of PR8 within respiratory epithelia or *in vitro*. Inflammation in coinfected mice remained focal compared to diffuse inflammation and damage in the lungs of mice infected by PR8. The timing of RV1B coinfection was a critical determinant of protection, suggesting that sufficient time is needed to induce this response. Finally, disease attenuation was not unique to RV1B: dose-dependent coinfection by a murine coronavirus (mouse hepatitis virus strain 1 [MHV-1]) also reduced the severity of PR8 infection. Unlike RV1B, coinfection with MHV-1 reduced early PR8 replication, which was associated with upregulation of beta interferon (IFN-β) expression. This model is critical for understanding the mechanisms responsible for influenza disease attenuation during coinfection by unrelated respiratory viruses.

IMPORTANCE Viral infections in the respiratory tract can cause severe disease and are responsible for a majority of pediatric hospitalizations. Molecular diagnostics have revealed that approximately 20% of these patients are infected by more than one unrelated viral pathogen. To understand how viral coinfection affects disease severity, we inoculated mice with a mild viral pathogen (rhinovirus or murine coronavirus), followed 2 days later by a virulent viral pathogen (influenza A virus). This model demonstrated that rhinovirus can reduce the severity of influenza A virus, which corresponded with an early but controlled inflammatory response in the lungs and early clearance of influenza A virus. We further determined the dose and timing parameters that were important for effective disease attenuation and showed that influenza disease is also reduced by coinfection with a murine coronavirus. These findings demonstrate that coinfecting viruses can alter immune responses and pathogenesis in the respiratory tract.

KEYWORDS coinfection, coronavirus, immunopathogenesis, influenza, mouse model, rhinovirus

Respiratory tract infections are a leading cause of morbidity and mortality worldwide, and viruses from many different families contribute to the disease burden. Advances in viral diagnostics and surveillance have led to the finding that viral

Received 18 May 2018 **Accepted** 13 September 2018

Accepted manuscript posted online 19 September 2018

Citation Gonzalez AJ, Ijezie EC, Balemba OB, Miura TA. 2018. Attenuation of influenza A virus disease severity by viral coinfection in a mouse model. J Virol 92:e00881-18. https://doi.org/10.1128/JVI.00881-18.

Editor Stacey Schultz-Cherry, St. Jude Children's Research Hospital

Address correspondence to Tanya A. Miura, tmiura@uidaho.edu.

coinfection or the presence of multiple unrelated viruses is quite common in the respiratory tract (1–4). Viruses involved in coinfections have the potential for interactions within the host that could affect replication dynamics, immune responses, and disease pathogenesis (5, 6). A substantial amount of research has focused on virus and bacterium coinfections (virus/bacterium coinfections), as it is common for a viral infection in the respiratory tract to enhance susceptibility of the host to a subsequent bacterial infection (7). However, much less is known about how coinfection by unrelated respiratory viruses affects pathogenesis.

Influenza viruses and rhinoviruses are common causes of both upper and lower respiratory tract infections across all age groups (4, 8–10). Thus, it is not surprising that they are frequently detected in coinfected patients. During the 2009 pandemic, the severity of influenza was reduced by coinfection with rhinoviruses, although it was enhanced by coinfection with other respiratory viruses (11). These differences did not correspond with changes in viral replication, as equivalent H1N1 viral loads were detected in coinfected patients and those infected by influenza A virus alone (11). Other clinical studies have found that respiratory viral coinfection can enhance (12–14), reduce (15, 16), or have no effect (17) on the severity of influenza. These differences may be due to the viruses involved, the order that they infected the host, and differences in patient populations. The disease severity of rhinovirus infections has also been shown to be affected by viral coinfections. Coinfection by influenza viruses has been found to reduce the severity of rhinovirus infection (13), and coinfection by respiratory syncytial virus enhances disease compared to that caused by rhinovirus alone (13, 18–20). Finally, epidemiological studies suggest that rhinoviruses may interfere with the spread of influenza within populations (10, 21–24). Likewise, spread of the 2009 pandemic H1N1 strain appears to have delayed the circulation of other seasonal respiratory viruses (9). One study found that influenza viruses and rhinoviruses were detected as copathogens less frequently than would be expected based on their detection rates within the population (4). This was also true for other virus pairs, including rhinoviruses with metapneumovirus or respiratory syncytial virus. In contrast, other pairs were detected as copathogens more frequently than expected, including rhinovirus with adenovirus and coronavirus with respiratory syncytial virus (4). Altogether, these studies suggest that respiratory viruses have complex interactions at the host and population levels. Model systems in which the viral strains and infection timing and doses are controlled are needed to understand these interactions at a mechanistic level.

In order to study the effects of viral coinfection on influenza disease pathogenesis, we established a mouse model of coinfection using mouse-adapted influenza A virus strain A/Puerto Rico/8/1934 (PR8). PR8 infection in BALB/c mice causes dose-dependent disease severity, in which mortality corresponds with early viral replication and cytokine production, followed by massive cellular infiltration in the lungs (25–27). To determine how PR8-mediated disease is altered by a mild viral infection, we coinfected mice with human rhinovirus strain 1B (RV1B) or a murine coronavirus, mouse hepatitis virus strain 1 (MHV-1). RV1B infects mice using low-density lipoprotein as its receptor, which is found on murine respiratory epithelial cells (28). Inoculation of BALB/c mice with an extremely high dose of RV1B results in neutrophil and lymphocyte recruitment to the airways, along with expression of antiviral and proinflammatory cytokines, without causing overt disease (29). MHV-1 is a respiratory tropic coronavirus that is a native pathogen of mice. While MHV-1 causes severe disease in A/J and Toll-like receptor 4 (TLR4)-deficient mouse strains, it causes dose-dependent severity in the respiratory tract of BALB/c mice (30, 31).

Here, we show that rhinovirus RV1B (RV) reduced the pathogenesis of influenza A virus PR8 infection and that the severity of PR8 infection and the timing of coinfection were critical determinants of disease attenuation. Coinfection-mediated protection corresponded with early but controlled pulmonary inflammation and enhanced recovery of coinfected mice. RV did not prevent infection by PR8 or inhibit early replication, but it did lead to faster clearance. Interestingly, attenuation of PR8 disease was not

limited to coinfection by RV, it was also seen when mice were coinfected by MHV-1 (MHV). Mice that were coinfected with MHV and PR8 had reduced levels of PR8 in the lungs early in infection, which corresponded with robust upregulation of beta interferon (IFN-β) expression. By identifying the parameters that are critical for disease attenuation during coinfection, such as viral doses, order, and timing of infection, we have established a model system in which we can determine how coinfecting viruses interact with the host's immune system to alter pathogenesis.

(This article was submitted to an online preprint archive [32].)

RESULTS

RV infection 2 days before PR8 lessens disease severity in mice. Patients that are coinfected by H1N1 influenza A virus and rhinovirus have less severe disease than those that are coinfected by H1N1 and other viruses (11). To evaluate the effects of rhinovirus coinfection on influenza disease severity, we inoculated mice with RV, followed 2 days later by a low, medium, or high dose of PR8 ($PR8_{Low}$, $PR8_{Med,}$ or $PR8_{Hi}$, respectively). Control groups were inoculated with RV and mock inoculated (RV/Mock) or mock inoculated and inoculated with PR8 (Mock/PR8) on day −2/day 0. The mice were monitored daily for mortality and weight loss and given a score based on clinical signs of disease, including ruffled fur, hunched posture, lethargy, and labored breathing. Humane endpoints included loss of more than 25% of their starting weight and/or severe clinical signs of disease. Similar to previous studies (29), mice inoculated with RV had no mortality or morbidity, including weight loss and clinical signs (Fig. 1A to C, RV/Mock). Mice that were inoculated with RV had no distinguishable differences in weight loss or clinical signs from mice that received mock inoculations (data not shown). Mice inoculated with $PR8_{Low}$ (Mock/$PR8_{Low}$) reached 40% mortality by day 8, but the remaining mice survived until the end of the study (Fig. 1A). These mice began losing weight and showing clinical signs on day 3, which progressed until the peak of disease on day 8 (Fig. 1B and C). Clinical signs of disease included minor ruffling of fur and hunching of the back, which progressed to include slightly labored breathing until eventual recovery from infection. In contrast to the mice infected with $PR8_{Low}$ alone, mice inoculated with RV 2 days before $PR8_{Low}$ (RV/$PR8_{Low}$) all survived until the end of the study (Fig. 1A). Coinfected mice lost weight between days 3 to 7, but the rate of loss and maximum weight loss were less than for mice infected by $PR8_{Low}$ alone (Fig. 1B). Clinical signs in coinfected mice were limited to minor ruffling and hunching, and the onset of these signs was delayed until day 5 compared to mice infected with a low dose of PR8 alone (Fig. 1C).

RV-mediated disease attenuation was less effective when the dose of PR8 was increased. Mice that were inoculated with a medium dose of PR8 (Mock/$PR8_{Med}$) had increased mortality, weight loss, and clinical signs compared to mice inoculated with Mock/$PR8_{Low}$. Furthermore, disease severity was only partially reduced by coinfection with RV (RV/$PR8_{Med}$). All mice inoculated with $PR8_{Med}$ alone succumbed to infection, whereas two of the seven coinfected mice survived (Fig. 1D). Both groups of mice, Mock/$PR8_{Med}$ and RV/$PR8_{Med}$, began losing weight on day 3, which continued until day 8 (Fig. 1E). Mice inoculated with $PR8_{Med}$ alone had more severe clinical signs throughout PR8 infection; they exhibited severe ruffling, mild lethargy, hunching, and labored breathing (Fig. 1F). In contrast, coinfected (RV/$PR8_{Med}$) mice had milder clinical signs limited to mild ruffling, slight hunching, and lethargy, which resolved as the surviving mice began to regain weight.

RV did not alter disease severity when mice were infected with a high dose of PR8. All mice inoculated with $PR8_{Hi}$ alone reached humane endpoints by day 7, 1 day earlier than mice inoculated with $PR8_{Med}$ (compare Fig. 1G and D). Mock/$PR8_{Hi}$-infected mice lost weight at a rate similar to that of mice inoculated with Mock/$PR8_{Med}$ (compare Fig. 1H and E) but displayed more severe clinical signs at later times in infection (compare Fig. 1I and F). Mock/$PR8_{Hi}$-infected mice had moderate ruffling and hunching on day 3, which quickly progressed to severe ruffling and hunching and moderate-severe lethargy and labored breathing before succumbing to infection (Fig. 1I). Coinfected mice

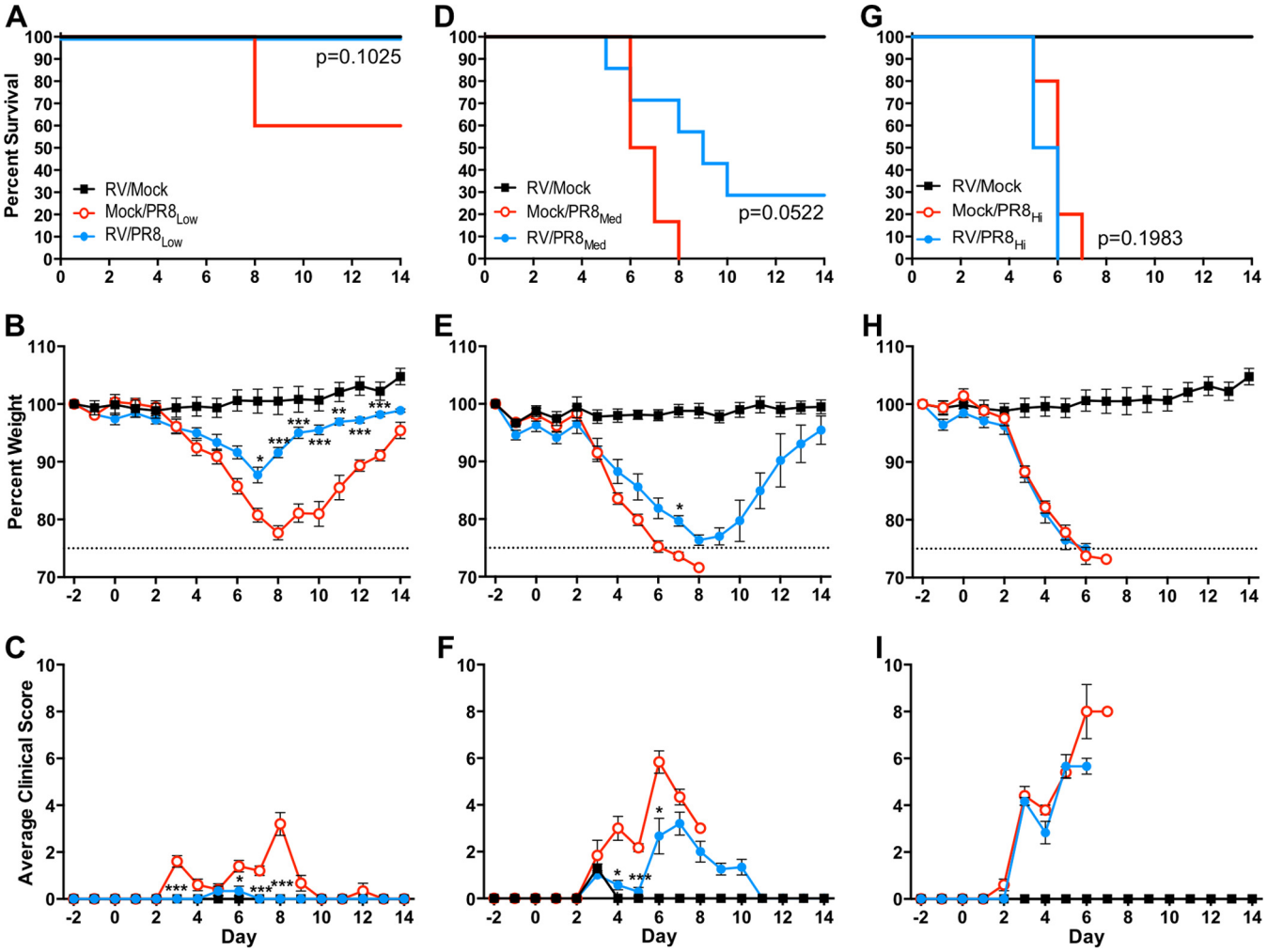

FIG 1 Disease kinetics in mice infected by influenza A virus PR8 or coinfected with rhinovirus (RV) 2 days before PR8. Mice were either mock inoculated or inoculated with 7.6×10^6 $TCID_{50}$ units of RV on day −2. On day 0, mice were either mock inoculated or inoculated with PR8 at ~100 ($PR8_{Low}$) (A to C), ~200 ($PR8_{Med}$) (D to F), or ~7.5×10^3 ($PR8_{Hi}$) (G to I) $TCID_{50}$ units. Mice were monitored for mortality (A, D, and G), weight loss (B, E, and H), and clinical signs of disease (C, F, and I), including lethargy, ruffled fur, hunched back, and labored breathing. Clinical scores were assigned on a scale of 0 to 3 in each category, and total daily scores were averaged. Values are means ± standard errors (error bars) for five to seven mice and are representative of two independent experiments. Survival curves were compared using log rank Mantel-Cox curve comparison, and *P* values for Mock/PR8 versus RV/PR8 are indicated. Weight loss and clinical score data were compared using multiple Student's *t* tests with Holm-Sidak multiple-comparison correction. Values for the RV/PR8 group that are significantly different from the values for the Mock/PR8 group are indicated by asterisks as follows: *, $P < 0.05$; **, $P < 0.01$; ***, $P < 0.001$.

($RV/PR8_{Hi}$) had no differences in mortality (Fig. 1G), weight loss (Fig. 1H), or clinical signs (Fig. 1I) compared to $Mock/PR8_{Hi}$-infected mice. In summary, RV lessened the severity of a mild or moderate, but not severe, infection by influenza A virus PR8 when inoculated 2 days before PR8.

Coinfection by RV leads to rapid clearance of PR8 from the lungs. The above-described experiments established that RV effectively attenuated disease upon infection with influenza A virus PR8. We next asked whether the reduced virulence during coinfection was due to inhibition of PR8 replication within the lungs. Groups of mice were either mock inoculated or inoculated with RV 2 days before inoculating with a low dose of PR8 (Mock/PR8 or RV/PR8, respectively). Groups of mice were euthanized on days 2, 4, 7, and 10 after PR8 inoculation, and lungs were harvested for PR8 quantification. On days 2 and 4 after PR8 inoculation, the viral loads in single-virus-infected and coinfected mice were not significantly different (Fig. 2A). However, on day 7, the Mock/PR8-infected mice still had PR8 titers in the 10^4 to 10^5 range, whereas the RV/PR8-coinfected mice had undetected levels of PR8. By day 10, both groups had undetected levels of infectious PR8. This suggests that coinfection with RV did not

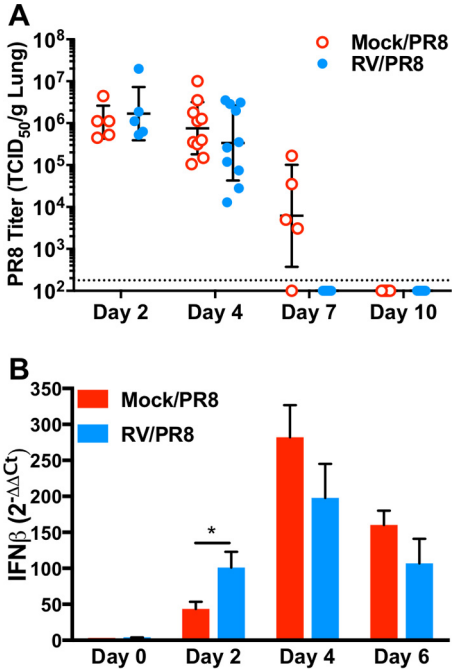

FIG 2 Influenza A virus PR8 titers and IFN-β expression in the lungs of mice infected by PR8 or coinfected by RV 2 days before PR8. Mice were either mock inoculated or inoculated with 7.6×10^6 $TCID_{50}$ units of RV on day -2. On day 0, mice were inoculated with ~100 $TCID_{50}$ units of PR8. (A) PR8 was titrated by $TCID_{50}$ assay of homogenized lungs. Data for individual mice are shown with the geometric mean standard deviation indicated for each group. The dotted line indicates the limit of detection of the assay. Titers were compared between groups using a Student's *t* test, which determined that they were not significantly different. (B) IFN-β expression was quantified by RT-qPCR. Threshold cycle (Ct) values were normalized to the values for GAPDH, and the fold change versus mock-inoculated mice was calculated. Mean values plus standard errors from five biological replicates are shown. Relative IFN-β levels were compared between groups using an unpaired *t* test, and values that are significantly different ($P < 0.05$) are indicated by a bar and asterisk.

prevent infection or inhibit early replication of PR8 but induced more rapid clearance of PR8 from the lungs. In agreement with other studies (29), RV was not detected in the lungs 2 days after inoculation (data not shown). Due to the rapid clearance of RV from the lungs of inoculated mice, we did not analyze RV titers at later time points.

To determine whether a type I interferon (IFN) response was associated with viral clearance, we quantified IFN-β mRNA in lungs from Mock/PR8- and RV/PR8-infected mice through the course of coinfection (Fig. 2B). Other studies have shown that IFN-β is significantly upregulated by RV1B infection of BALB/c mice on day 1 after infection but is nearly back to baseline levels by day 2 (29). Similarly, IFN-β expression was not significantly upregulated compared to mock inoculation on day 0, which is 2 days after RV infection (Fig. 2B). However, IFN-β mRNA levels in RV/PR8-coinfected mice were significantly higher than those in Mock/PR8-infected mice on day 2. Although it was not statistically significant, there was a trend toward reduced IFN-β in coinfected mice on days 4 and 6.

We also evaluated lung sections for influenza A virus PR8 antigens by immunohistochemistry. The lack of PR8 antigen staining in lung sections from mock-inoculated mice confirmed the specificity of staining (Fig. 3A). On day 4, both single-virus- and coinfected groups had extensive infection of the tracheal and bronchial epithelium (not shown) in addition to viral antigen in bronchiolar epithelia and alveoli (Fig. 3B). Although the bronchiolar epithelial cells from both groups contained viral antigen, the Mock/PR8-infected lung tissues had more extensive sloughing of infected epithelia with viral antigen associated with mucopurulent material in the airways. Both groups had focal viral antigen staining in the alveoli, with antigen detected in pneumocytes and immune cells, especially macrophages and neutrophils. On day 7, antigen staining was

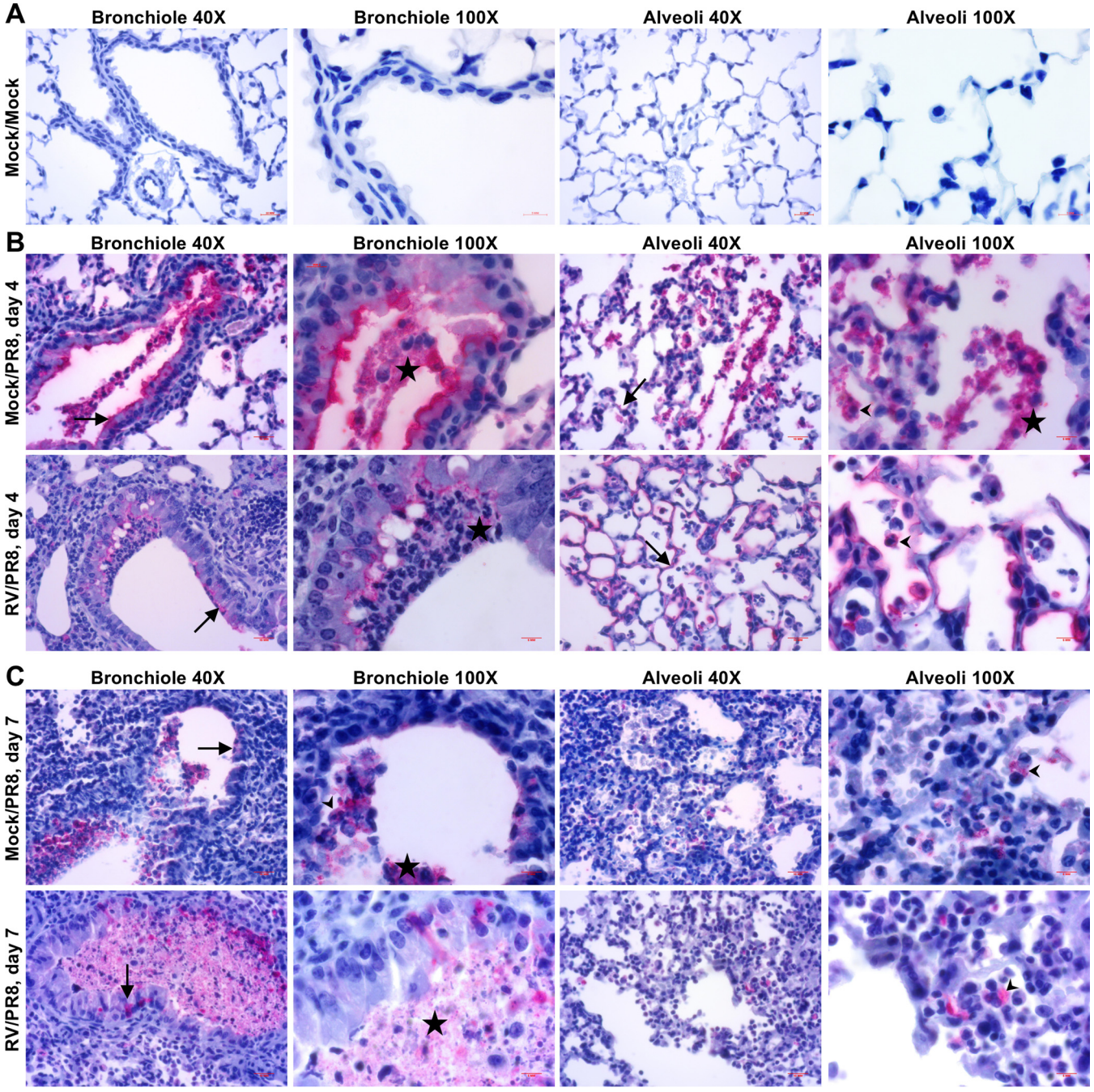

FIG 3 Immunohistochemistry of PR8 antigen in the lungs of mice infected by influenza A virus PR8 or coinfected with RV 2 days before PR8. Images taken of the indicated regions of the lungs and at the indicated magnifications show mice given mock inoculations on days −2 and 0 (A) and mice given Mock/PR8 or RV/PR8 on day −2/day 0 (B and C). Tissue sections were immunostained for the PR8 hemagglutinin protein, which was visualized by ImmPACT Vector red, and counterstained with hematoxylin. Lung tissues were collected on day 4 (B) and day 7 (C) after PR8 inoculation. Images were representative of two sections from two animals per group and time point. Examples of antigen in epithelial cells (black arrows), antigen in leukocytes (predominantly macrophages and neutrophils) (black arrowheads), and mucopurulent material (black stars) are indicated.

reduced in lung tissues from both groups and was localized in airways, especially cells that had been sloughed from the epithelium (Fig. 3C). PR8 antigens in the alveoli were mainly found in immune cells by day 7, suggesting clearance of infection. In agreement with the undetected levels of infectious PR8, both groups had little antigen staining on day 10, which was predominantly in immune cells within focal areas (not shown). These findings support our observation that coinfection by RV did not prevent replication of PR8 in the respiratory tract.

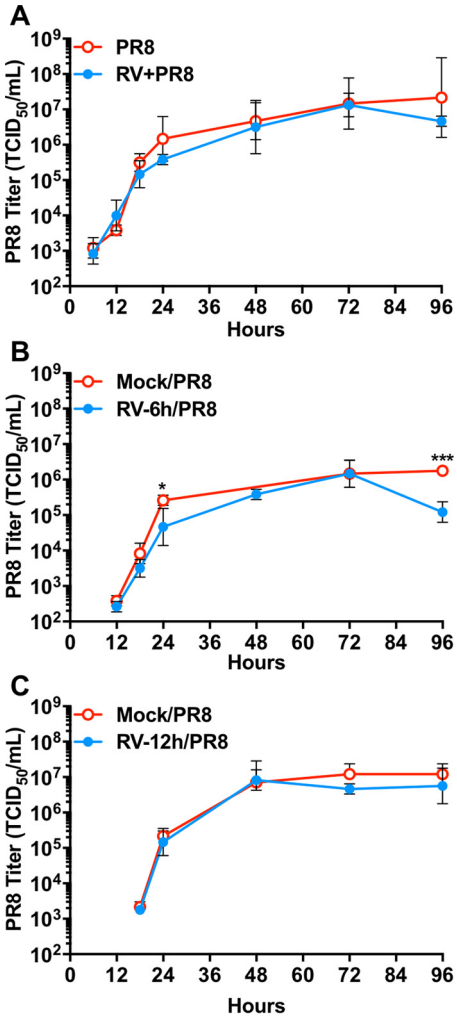

FIG 4 Growth curves of influenza A virus PR8 from cells infected by PR8 or RV and PR8. LA-4 cells were inoculated with RV (MOI of 1) simultaneously (A) or 6 h (B) or 12 h (C) before inoculation with PR8 (MOI of 1). Media were collected at the indicated times after PR8 inoculation and titrated for PR8 by $TCID_{50}$ assay. Data shown are geometric means ± standard deviations from three samples per group and time point and are representative of two replicate experiments. Values that are significantly different from the values for the Mock/PR8 group were determined by Student's *t* test and are indicated by asterisks as follows: *, $P < 0.05$; ***, $P < 0.001$.

RV does not interfere with replication of PR8 *in vitro*. Next, we used a murine lung epithelial cell line (LA-4) that is susceptible to infection by both viruses (33) to determine whether coinfection by RV would interfere with PR8 replication *in vitro*. LA-4 cells were inoculated with RV 6 or 12 h before or simultaneously with influenza A virus PR8. PR8 released into the media was quantified by 50% tissue culture infective dose ($TCID_{50}$) assay in MDCK cells. We confirmed that the presence of RV in these samples did not interfere with quantification of PR8 in MDCK cells (not shown). There were no significant differences at any time point between cells inoculated with PR8 alone or coinfected with RV either simultaneously with or 12 h before PR8 (Fig. 4A and C). There were significant differences at 24 and 96 h when cells were inoculated with RV 6 h before PR8 (Fig. 4B). The lower PR8 titers at 96 h may have been due to higher cell death from two viruses being present, providing fewer susceptible cells for PR8 replication. Although it was not significant, this trend was also seen when cells were inoculated with both viruses simultaneously (Fig. 4A). These data help corroborate our *in vivo* finding that RV did not inhibit replication of PR8. Rather, coinfection is most likely stimulating the immune system, leading to faster clearance of PR8.

Coinfection with RV stimulated an early yet controlled inflammatory response to PR8 infection. We next evaluated the histopathology of lungs from mice infected with a single virus (Mock/PR8) and coinfected mice (RV/PR8) on days 4, 7, and 10 after inoculation with influenza A virus PR8. Compared to mock-inoculated controls, both Mock/PR8- and RV/PR8-infected mice had multifocal tracheobronchitis and bronchioalveolitis (Fig. 5A to C and data not shown). Lung pathology was characterized by epithelial degeneration, necrosis, and sloughing and accumulation of neutrophils, macrophages, and lymphocytes in the inflamed areas. This was associated with the accumulation of mucopurulent discharge in the bronchioles and alveoli (Fig. 5C). The extension of inflammation from bronchioles into the surrounding lung parenchyma resulted in localized alveolitis. In general, inflammation was associated with dilated and congested blood capillaries with extravasation of blood plasma, hemorrhage, thickened alveolar septae, collapsed alveoli, and enlarged alveolar ducts observed in severe lesions (Fig. 5B and C). Although focal inflammation was found in all lobes, the right lung's caval lobe appeared to be commonly more inflamed than other lobes. Pulmonary invagination was often associated with inflamed portions of the lungs.

Coinfection with RV induced earlier inflammation but reduced the severity of inflammation elicited by influenza A virus PR8. By day 4, lung pathology was more extensive in RV/PR8-coinfected mice than in Mock/PR8-infected mice. However, by days 7 and 10, mice infected with Mock/PR8 had more severe lung pathology than RV/PR8-coinfected mice. Overall, necrosis and desquamation in the trachea, bronchi, bronchioles, and alveoli were more severe in Mock/PR8-infected mice than in RV/PR8-coinfected mice. Furthermore, excessive mucopurulent material consisting of neutrophils, macrophages, cellular debris, and transudate accumulated in the lungs of Mock/PR8-infected mice. Congestion and hemorrhage were also more severe, and pleurisy was present only in the lungs of Mock/PR8-infected mice. The expansion of bronchiolar inflammation into the parenchyma and collapse and destruction of alveoli was less extensive in the lungs of RV/PR8-coinfected mice. Note that perivascular cuffing was more dense and widespread in RV/PR8-coinfected mice, and their lungs had more lymphocytes and macrophages and fewer neutrophils than the lungs of Mock/PR8-infected mice. These findings suggest that Mock/PR8-infected mice had more tissue damage and exacerbated inflammation, while RV/PR8-coinfected mice had a more focused antiviral cellular immune response. Serial imaging and estimation of inflamed areas, which was performed in a blind manner, were done using ImageJ software. The results of this analysis are summarized in Fig. 5B, which shows that lung sections from RV/PR8-coinfected mice had inflammation over 60% to 79% of the tissue on day 4, which declined to 40% to 59% on days 7 and 10. In contrast, sections from Mock/PR8-infected mice had lower levels of inflammation ($<$20%) on day 4 but higher levels of inflammation on days 7 ($>$80%) and 10 (60% to 79%).

Coinfection by RV also resulted in earlier resolution of inflammation and tissue regeneration. Type II pneumocyte hyperplasia and regeneration of the epithelium were observed in the bronchioles and alveoli of RV/PR8-coinfected mice on days 7 and 10; these are signs of regeneration. Overall, there were fewer inflammatory cells in the alveoli in lungs of RV/PR8-coinfected mice compared with lungs of Mock/PR8-infected mice. Pleurisy was encountered in some of the lungs obtained from Mock/PR8-infected mice but not in RV/PR8-coinfected mice. In summary, the findings of this study show that coinfecting mice with RV reduced the magnitude of the inflammatory response to PR8 infection and accelerated epithelial repair and alveoli restoration and the overall recovery.

The timing of RV coinfection determines the effect on disease severity during PR8 infection. Coinfection by RV was effective at reducing disease severity when given 2 days before a low or medium dose of influenza A virus PR8. We next determined whether coinfection with RV simultaneously with or 2 days after a low or medium dose of PR8 would also ameliorate disease. When RV and $PR8_{Low}$ were inoculated simultaneously (RV+$PR8_{Low}$), coinfection resulted in a disease phenotype intermediate between $PR8_{Low}$ alone (Mock/$PR8_{Low}$) and RV 2 days before $PR8_{Low}$ (RV/$PR8_{Low}$) (Fig. 6A

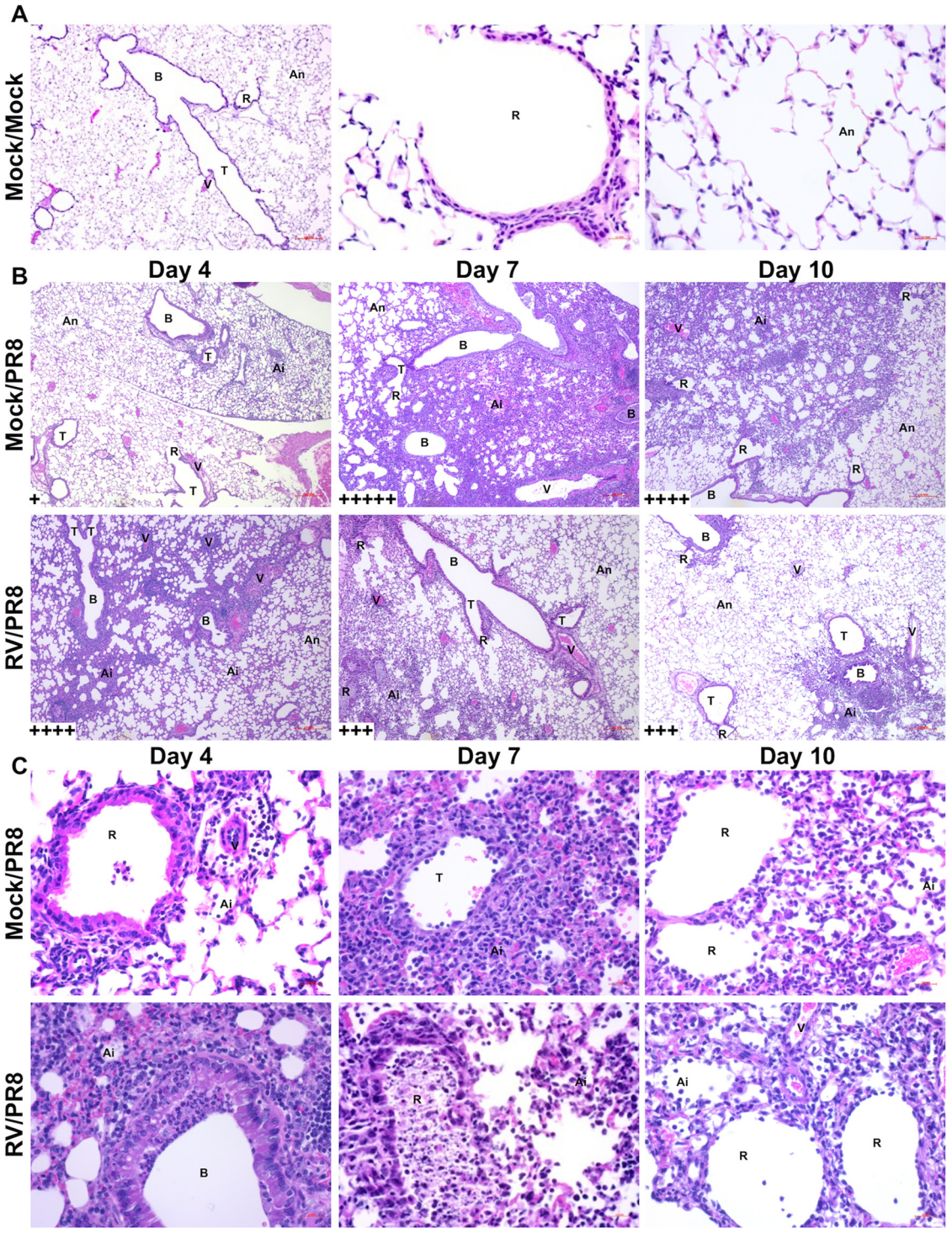

FIG 5 Histopathology of mouse lungs infected by influenza A virus PR8 or coinfected with RV 2 days before PR8. Mice were either mock inoculated or inoculated with 7.6×10^6 $TCID_{50}$ units of RV on day −2. On day 0, mice were either mock inoculated or inoculated with ~100 $TCID_{50}$ units of PR8. Lungs were embedded in paraffin, and sections were stained with hematoxylin and eosin. Images were representative of two tissue sections from two mice per group and time point. (A) Images from lung sections of Mock/Mock-inoculated mice taken with 10× and 40× objectives. (B) Images from the indicated groups and days taken with a 10× objective. (C) Images from the indicated groups and days taken with a 40× objective. Inflammation was scored in a blind manner by estimating the percentage of inflamed area using serial imaging and ImageJ software. Sections were assigned scores based on the average percentage of inflamed area across replicates as indicated in the lower left corners of images in panel B: <20% (+), 20% to 39% (++), 40% to 59% (+++), 60% to 79% (++++), and >80% (+++++). Labeled structures include bronchioles (B), terminal bronchioles (T), respiratory bronchioles (R), normal alveoli (An), inflamed alveoli (Ai), and blood vessels (V).

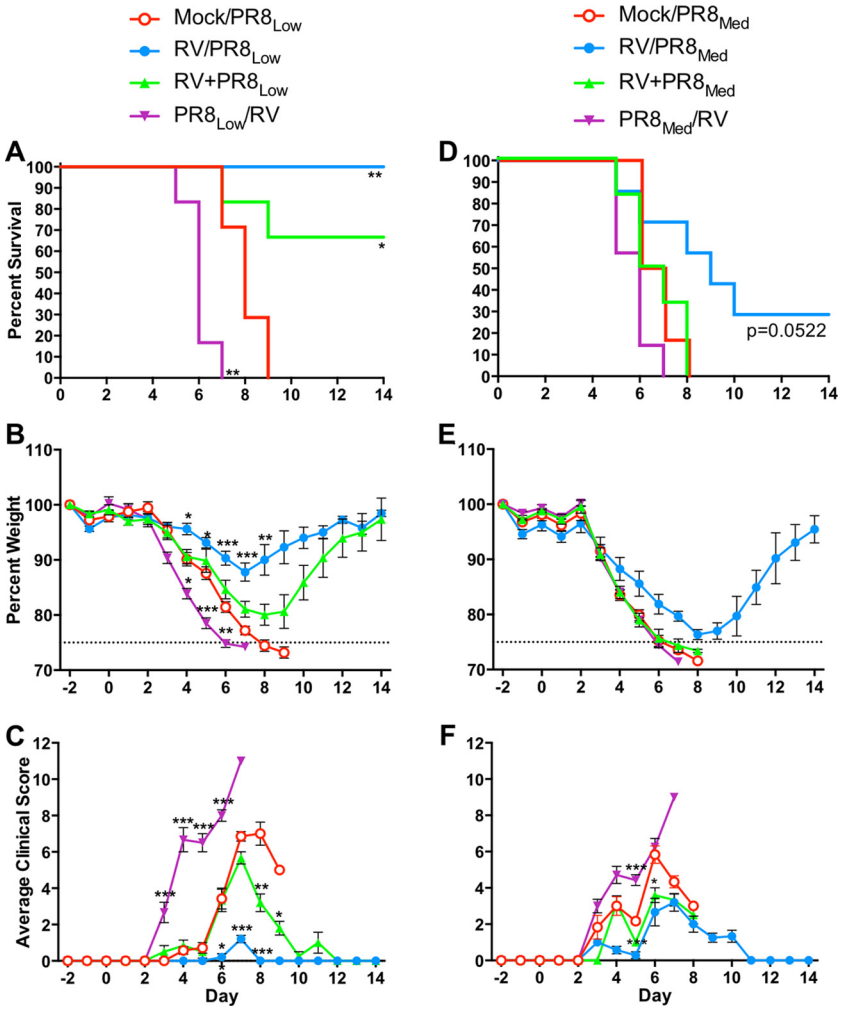

FIG 6 Disease kinetics in mice coinfected by RV 2 days before, simultaneously with, or 2 days after PR8 infection. Groups of six or seven mice were either mock inoculated or inoculated with 7.6×10^6 $TCID_{50}$ units of RV 2 days before (RV/PR8), simultaneously with (RV+PR8), or 2 days after (PR8/RV) inoculation with ~100 ($PR8_{Low}$) or ~200 ($PR8_{Med}$) $TCID_{50}$ units of PR8. Mice were monitored for mortality, weight loss, and clinical signs of disease (lethargy, ruffled fur, hunched posture, and labored breathing) for 14 days after PR8 inoculation. (A to C) RV and low-dose PR8 coinfection mortality (A), weight loss (B), and clinical scores (C). (D to F) RV and medium-dose PR8 coinfection mortality (D), weight loss (E), and clinical scores (F). Survival curves were compared using log rank Mantel-Cox curve comparison. Weight loss and clinical score data were compared using multiple Student's *t* tests with Holm-Sidak multiple-comparison correction. Values that are significantly different from the values for the Mock/PR8 group are indicated by asterisks as follows: *, $P < 0.05$; **, $P < 0.01$; ***, $P < 0.001$.

to C). RV+$PR8_{Low}$-coinfected mice reached 33% mortality by day 9 (Fig. 6A). This mortality was higher than mice inoculated with RV 2 days before $PR8_{Low}$ (RV/$PR8_{Low}$) but significantly lower than the 100% mortality seen with mice infected with $PR8_{Low}$ alone (Mock/$PR8_{Low}$). RV+$PR8_{Low}$-infected mice lost weight at a rate similar to that of Mock/$PR8_{Low}$-infected mice, beginning on day 3 and continuing until day 8 before recovering (Fig. 6B). Average clinical scores were also similar between simultaneous coinfection and single infection, with slight lethargy, hunching, labored breathing, and moderate ruffling detected on days 3 and 4 and peaking with moderate lethargy, hunching, labored breathing, and severe ruffling on day 7 before coinfected mice (RV+$PR8_{Low}$) began recovering from infection (Fig. 6C). Interestingly, when RV was given 2 days after $PR8_{Low}$ ($PR8_{Low}$/RV), coinfection exacerbated PR8 disease, as evidenced by more rapid mortality, weight loss, and higher clinical scores than for mice infected with Mock/$PR8_{Low}$ (Fig. 6A to C). $PR8_{Low}$/RV-coinfected mice began dying and

reached 100% mortality 2 days before mice inoculated with Mock/$PR8_{Low}$ (Fig. 6A). $PR8_{Low}$/RV-coinfected mice also lost weight at a greater rate and had dramatically higher clinical scores than other single-virus-infected and coinfected groups (Fig. 6B and C). These increased clinical scores were due to severe lethargy and ruffling, moderate hunching, and labored breathing, which occurred earlier during infection than in mice in the other groups (Fig. 6C).

In contrast to $PR8_{Low}$, RV was effective at disease attenuation only when given 2 days before a higher dose ($PR8_{Med}$) of PR8. There were no significant differences in mortality, weight loss, or clinical signs between simultaneously coinfected (RV+$PR8_{Med}$) mice and mice inoculated with $PR8_{Med}$ alone (Fig. 6D to F). Both of these groups steadily lost weight between days 3 to 8 and reached 100% mortality by day 8 (Fig. 6D and E). RV+$PR8_{Med}$-coinfected mice had slightly lower clinical scores than Mock/$PR8_{Med}$-infected mice (Fig. 6F) and did not experience severely labored breathing like Mock/$PR8_{Med}$-infected mice. However, these differences in clinical signs did not affect mortality. When RV was inoculated 2 days after $PR8_{Med}$ ($PR8_{Med}$/RV), all mice reached humane endpoints by day 7, 1 day earlier than mice inoculated with Mock/$PR8_{Med}$ (Fig. 6D). $PR8_{Med}$/RV-coinfected mice lost weight at a rate similar to that of Mock/$PR8_{Med}$-infected mice and had similar clinical scores (Fig. 6E and F). These data demonstrate that RV provides protection from PR8-induced disease in a time-dependent manner. Disease attenuation was most effective when RV had adequate time to activate a protective response.

Disease attenuation is not limited to coinfection by RV. We next evaluated whether attenuation of PR8 disease was limited to coinfection by RV or whether a different respiratory virus would also be effective. Mice were either mock inoculated or inoculated with MHV 2 days before influenza A virus PR8 and monitored for survival and weight loss over 14 days. One mouse inoculated with 2×10^3 PFU of MHV (MHV_{2000}/Mock) reached a humane endpoint, but the remaining mice survived until the end of the study (Fig. 7A). MHV-infected mice (MHV_{2000}/Mock) had rapid, early weight loss followed by gradual recovery of weight (Fig. 7B). These mice had moderate ruffling and hunching early in infection, which decreased to slight ruffling, lethargy, and hunching before the mice finally recovered on day 13 (Fig. 7C). Despite the prolonged morbidity in MHV-infected mice, the mortality and morbidity of mice coinfected with a lethal dose of PR8 (MHV_{2000}/PR8) were similar to the mortality and morbidity of mice infected by MHV alone (Fig. 7A to C). MHV_{2000}/PR8-coinfected mice regained weight at a rate lower than that of mice inoculated with MHV_{2000}/Mock, but they eventually reached the same weight (Fig. 7B). Thus, coinfection by MHV reduced the severity of PR8-induced disease, but this dose of MHV caused significant morbidity in BALB/c mice.

To determine whether infection by a lower dose of MHV would cause less disease but still provide protection against influenza A virus PR8, we tested two additional doses of MHV: 1×10^3 PFU (MHV_{1000}) and 2×10^2 PFU (MHV_{200}). When mice were inoculated with the twofold-lower dose of MHV (MHV_{1000}/Mock), there was no mortality associated with infection (Fig. 7D). These mice lost weight very early in infection but did not lose as much weight as those infected by the higher dose (compare Fig. 7E and B). MHV_{1000}/Mock-infected mice had minor ruffling and hunching on day 0, which continued until day 9 (Fig. 7F). When MHV was inoculated 2 days before PR8 (MHV_{1000}/PR8), only one mouse reached a humane endpoint, and mortality was delayed until day 8, compared to day 5 for the higher dose of MHV (compare Fig. 7D and A). Similar to mice infected by MHV_{1000} alone, MHV_{1000}/PR8-coinfected mice lost weight early. However, coinfected mice had delayed recovery of weight, and their weight was still lower than MHV_{1000}-infected mice at the end of the study (Fig. 7E), which corresponded with prolonged clinical signs of disease (Fig. 7F). Although this lower dose of MHV caused milder infection and provided similar protection against PR8-mediated mortality, morbidity was prolonged in the coinfected mice, which suggests that it was less effective than the higher dose.

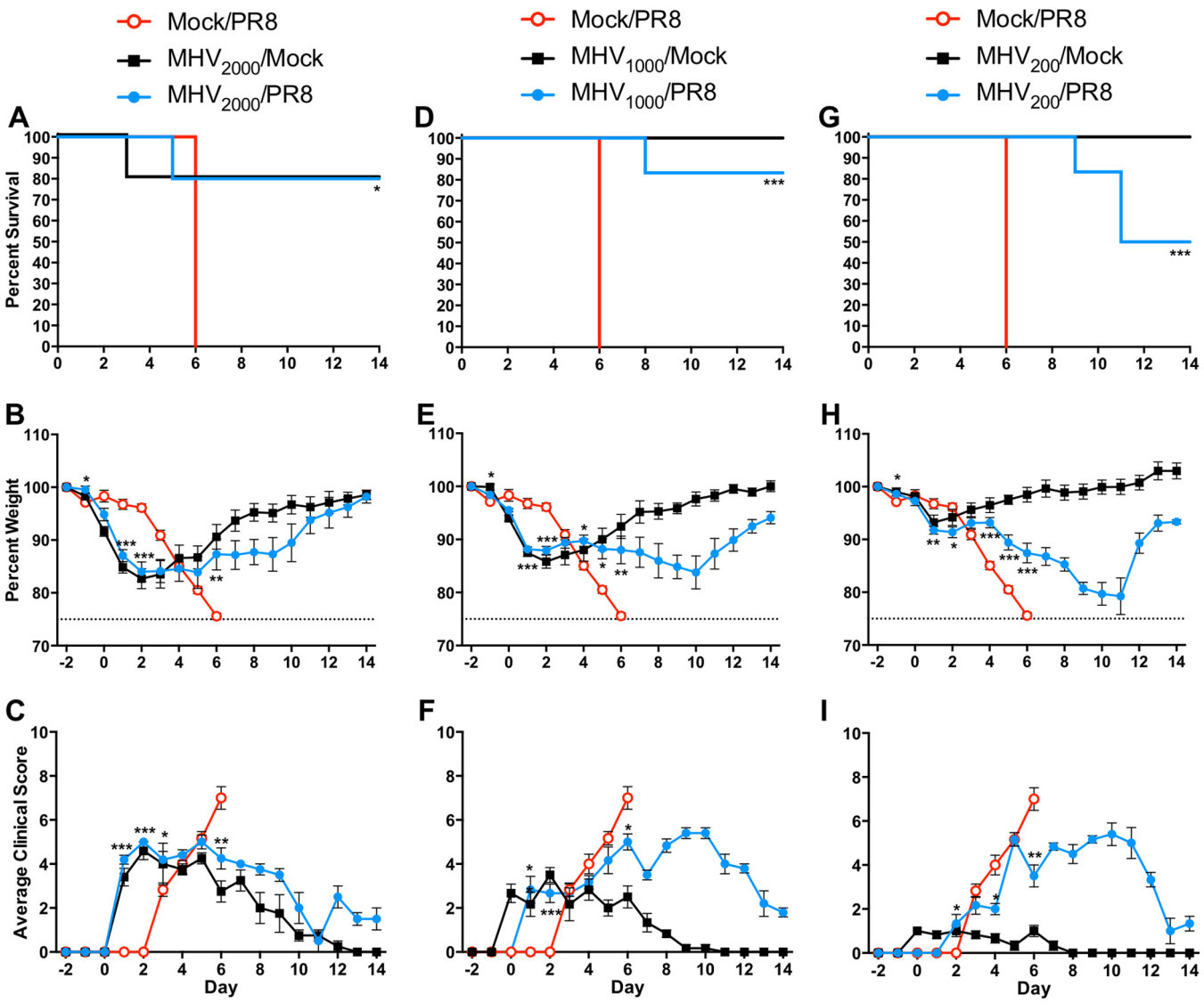

FIG 7 Disease kinetics in mice coinfected by MHV 2 days before influenza A virus PR8. Groups of five or six mice were either mock inoculated or inoculated with 2.0×10^3 (MHV_{2000}), 1.0×10^3 (MHV_{1000}), or 2.0×10^2 (MHV_{200}) PFU of MHV 2 days before inoculation with ~100 $TCID_{50}$ units of PR8. Mice were monitored for mortality, weight loss, and clinical signs of disease (lethargy, ruffled fur, hunched posture, and labored breathing) for 14 days after PR8 inoculation. (A to C) MHV_{2000} and PR8 coinfection mortality (A), weight loss (B), and clinical scores (C). (D to F) MHV_{1000} and PR8 coinfection mortality (D), weight loss (E), and clinical scores (F). (G to I) MHV_{200} and PR8 coinfection mortality (G), weight loss (H), and clinical scores (I). Survival curves were compared by using log rank Mantel-Cox curve comparison. Weight loss and clinical score data were compared by multiple Student's *t* tests with Holm-Sidak multiple-comparison correction. Values that are significantly different compared to the values for the Mock/PR8 group are indicated by asterisks as follows: *, $P < 0.05$; **, $P < 0.01$; *** $P < 0.001$.

When mice were inoculated with a 10-fold-lower dose of MHV (MHV_{200}/Mock), they all survived and had minimal weight loss and clinical signs of disease, which was limited to slight ruffling (Fig. 7G to I). However, mice that were coinfected with this low dose of MHV prior to PR8 (MHV_{200}/PR8) had significant mortality, weight loss, and prolonged clinical signs of disease, including moderate lethargy and labored breathing. Even though this lowest dose of MHV caused minimal disease in BALB/c mice, it was not as effective at reducing PR8-induced morbidity and mortality. These data suggest that a dose of MHV that causes significant morbidity is required to effectively protect against a lethal dose of influenza A virus PR8. Although both RV and MHV given 2 days earlier reduced the severity of PR8, they vary in pathogenesis and effectiveness of disease attenuation.

Coinfection by MHV reduces PR8 titers in lungs early in infection, which corresponds with upregulation of IFN-β expression. The lungs of Mock/PR8- and

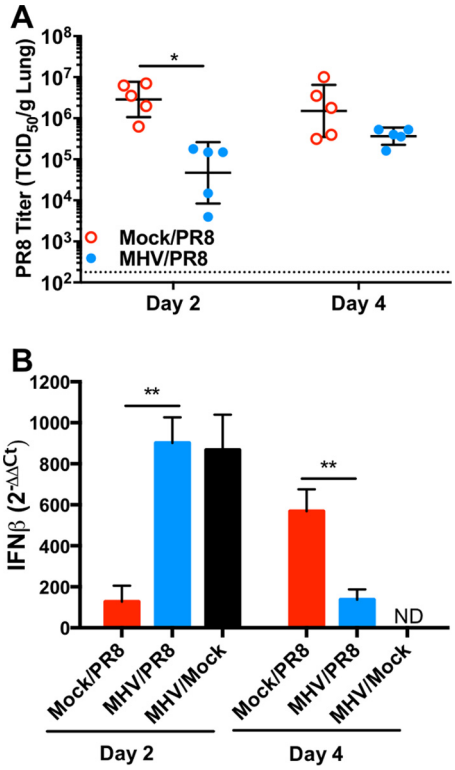

FIG 8 PR8 titers and IFN-β expression in the lungs of mice infected by influenza A virus PR8 or coinfected by MHV 2 days before PR8. Mice were either mock inoculated or inoculated with 2.0×10^3 PFU of MHV on day -2. On day 0, mice were inoculated with ~100 $TCID_{50}$ units of PR8 or were mock inoculated. (A) PR8 was titrated by the $TCID_{50}$ assay of homogenized lungs. Data for individual mice are shown with the geometric mean and standard deviation indicated for each group. The dotted line indicates the limit of detection of the assay. (B) IFN-β expression was quantified by RT-qPCR. Threshold cycle (Ct) values were normalized to GAPDH values, and the fold change values compared to the values for mock-inoculated mice were calculated. Mean values and standard errors from four biological replicates are shown. Values that are statistically significantly different for the Mock/PR8 and MHV/PR8 groups by an unpaired *t* test are indicated by asterisks as follows: *, $P < 0.05$; **, $P < 0.01$. ND, not determined.

MHV/PR8-infected mice were collected on days 2 and 4 after influenza A virus PR8 inoculation for quantification of PR8. In contrast to RV, coinfection by MHV 2 days before PR8 resulted in significantly lower replication of PR8 in the lungs on day 2 (Fig. 8A). PR8 loads in Mock/PR8- and MHV/PR8-infected groups were not significantly different on day 4. MHV titers were equivalent in mice infected with MHV alone or MHV/PR8-coinfected mice on day 2 (data not shown). To determine whether expression of IFN-β corresponds with reduced PR8 titers and disease severity in MHV/PR8-coinfected mice, IFN-β mRNA was quantified by reverse transcription-quantitative PCR (RT-qPCR). MHV/Mock- and MHV/PR8-infected groups had significantly increased IFN-β expression compared to Mock/PR8-infected mice on day 2 (Fig. 8B). On day 4, when IFN-β expression was upregulated in Mock/PR8-infected mice, expression of IFN-β was reduced in MHV/PR8-coinfected mice. These data demonstrate that MHV induces early upregulation of IFN-β that corresponds with reduced PR8 replication on day 2. However, the upregulation of IFN-β and reduction in PR8 replication was not sustained.

DISCUSSION

Clinical studies have suggested that respiratory viral coinfections may alter pathogenesis compared to infection by the viruses individually. Rhinovirus has been implicated in both interfering with the spread of influenza viruses and reducing the severity of influenza during coinfection (10, 11, 21–24). Here, we developed a murine model of respiratory viral coinfection to study the effects on disease severity in a system where we can control the virus strains, doses, order, and timing of when the viruses infect the

host. We found that mice given RV 2 days before influenza A virus PR8 were completely protected against mortality and had reduced morbidity. RV was less effective at disease attenuation when mice were given higher doses of PR8, or RV was given at the same time as PR8. While protective when given before PR8, RV enhanced disease when given 2 days after PR8, suggesting that RV-induced immune responses can be detrimental later during coinfection. We also found that disease attenuation was not limited to coinfection by RV. A respiratory tropic strain of MHV also reduced PR8 disease when given 2 days before PR8. Unlike RV, MHV caused significant morbidity in mice. However, reducing the dose of MHV to lessen pathogenesis was less effective at reducing the severity of PR8. These data suggest that changes in pathogenesis during coinfection are dependent upon the severity of each infection and the order and timing of inoculation. The dose, order, and timing of infection are rarely known during coinfections in humans; therefore, mouse models are critical to decipher the underlying mechanisms of pathogenesis.

Despite preventing mortality and significantly inhibiting morbidity, infection of mice with RV 2 days before PR8 did not reduce PR8 levels in the lungs early in infection (Fig. 2) or prevent spread of PR8 within the respiratory tract (Fig. 3). Similarly, treatment of mice with a live attenuated vaccine strain of *Bordetella pertussis* or Toll-like receptor (TLR) agonists prior to influenza A virus (IAV) reduces the severity of IAV infection without affecting viral titers in the lungs (34, 35). In contrast, treatment of mice with a double-stranded RNA (dsRNA) mimic prior to IAV infection significantly reduces viral load on day 3 (36). Our findings suggest that RV does not directly inhibit infection by PR8, which was also confirmed by our *in vitro* studies (Fig. 4). Other studies have shown that coinfection of cells by IAV and respiratory syncytial virus (RSV) simultaneously does not inhibit replication of IAV (37). However, they found that inoculation of IAV 12 h after RSV significantly lowered IAV titers, suggesting that depletion of target cells, and not direct interference, was responsible (37). In contrast, *in vitro* coinfection by parainfluenza virus (parainfluenza virus type 2 [PIV2]) has been shown to enhance IAV infection, which is dependent on the cell-cell fusion activity of PIV2 (38). Our previous studies have shown that RV induces a robust type I IFN response in the LA-4 cell line (33); thus, the lack of PR8 inhibition *in vitro* is likely not due to the absence of an IFN response. This is not surprising, as the NS1 protein of PR8 is known to antagonize type I IFN responses (39). Others have shown that RV induces expression of type I and type III IFNs in the respiratory tracts of infected mice (29, 40, 41). We further showed that RV/PR8-infected mice had increased IFN-β expression early in coinfection (day 2), which was not sufficient to reduce PR8 replication in the lungs at early time points (Fig. 2). Although our data do not support a role for RV-induced IFN responses in preventing infection by PR8, IFN may be important for inducing downstream antiviral responses that contribute to earlier clearance of PR8 in coinfected animals. In addition to promoting cell-intrinsic antiviral defense strategies, type I IFNs are important for the recruitment and functional phenotypes of myeloid cell responses to influenza virus infections (42, 43). In the absence of type I IFN signaling, PR8 disease severity is increased, but the enhanced disease is not completely due to increased viral loads. Rather, these studies showed that type I IFN signaling is needed to downregulate inflammatory monocyte and neutrophil responses during PR8 infection. Furthermore, in the absence of type I IFN signaling, monocytes develop increased inflammatory phenotypes and reduced expression of genes that downregulate inflammation (42, 43). Thus, type I IFN responses induced by RV could promote the downregulation of inflammation that we observed on days 7 and 10. Interestingly, there was a trend toward lower IFN-β expression by day 4 in coinfected animals despite high viral loads (Fig. 2). This may reflect active downregulation of innate responses by RV.

Histopathology analyses demonstrated that mice inoculated with RV 2 days before influenza A virus PR8 had earlier recruitment of immune cells into the lungs (Fig. 5). On day 4 after PR8 infection, coinfected animals had multiple foci of inflammation throughout the lungs. In contrast, animals infected with PR8 alone had reduced recruitment of inflammatory cells. This early immune response may lead to earlier clearance of PR8

from coinfected lungs, as we saw by day 7 (Fig. 2). Although RV (strain 1B) is not virulent in mice, it induces an inflammatory response in the respiratory tracts of BALB/c and C57BL/6 mice. The response to RV includes recruitment of neutrophils and lymphocytes, concurrent with production of antiviral cytokines and chemokines. Neutrophil levels in the airways of RV-infected mice peak on days 1 and 2 and decline by day 4, while lymphocytes are present through day 7 (29, 40, 41, 44, 45). Studies differ in whether macrophage numbers change significantly upon RV infection in mice (29, 40, 41, 44). Type I and III interferons, proinflammatory cytokines, and neutrophil- and lymphocyte-recruiting chemokines are also upregulated in response to RV infection in mice (29, 40, 41). These cellular and cytokine responses are not stimulated by UV-inactivated virus, suggesting that viral replication is required (29, 41). We observed increased macrophages and lymphocytes and enhanced perivascular cuffing in histology sections from RV/PR8-coinfected animals, suggesting a robust cellular immune response. Ongoing studies in our lab will determine the RV-induced immune components that are required for attenuation of PR8 disease during coinfection.

In contrast to the enhanced inflammation in the lungs of coinfected mice on day 4, the histopathology on days 7 and 10 was less severe in coinfected mice than in PR8-infected mice (Fig. 5). This could be an indirect consequence of early viral clearance (Fig. 2) or active downregulation of the inflammatory response in coinfected animals. Multiple studies have shown that inflammation during influenza and other respiratory viral infections can cause pathogenesis that is independent of viral levels in the lungs (42, 43, 46–48). Our histopathology data are in agreement with studies that demonstrate excessive inflammatory responses occurring as viral loads are decreasing (25, 49). We inoculated mice with influenza A virus PR8 2 days after RV inoculation, which is just prior to the decline in neutrophil numbers in the lungs of RV-infected BALB/c mice (29). Furthermore, RV infection actively downregulates neutrophil responses by inhibiting TLR signaling and thereby reducing expression of neutrophil-specific chemokines upon coinfection by a bacterial pathogen (50). The inflamed areas of the RV/PR8-coinfected lungs contained fewer neutrophils than Mock/PR8-infected lungs. Neutrophils are known to contribute to immune-mediated damage during PR8 infection (51, 52). Thus, active downregulation of neutrophilic inflammation by RV may contribute to the reduced severity of PR8 in our studies. Similar to our findings, the protective response against IAV induced by live attenuated *B. pertussis* is associated with lower levels of proinflammatory cytokines and recruitment of neutrophils into the airways without altering the level of infectious virus (34).

RV-mediated disease attenuation was less effective as we increased the dose of influenza A virus PR8, shortened the timing between virus inoculations, or gave RV after PR8 (Fig. 1 and 6). These differences are likely due to the kinetics and magnitudes of RV- and PR8-induced immune responses. Higher doses of PR8 likely overwhelm defense mechanisms that are induced by RV, and these defense mechanisms are likely not induced quickly enough to completely protect against PR8 given at the same time. However, the observation that RV given 2 days after PR8 exacerbates pathogenesis suggests that once a response to PR8 has been initiated, the RV-induced response may aggravate immunopathology. RV induces multiple immune components that are known to contribute to influenza disease, including neutrophils (51), NK cells (53), and type I IFNs (54, 55). Further studies are needed to identify the mechanisms that exacerbate disease when RV is given 2 days after PR8. It is possible that these are the same mechanisms that reduce disease when RV is given 2 days before PR8 and that the timing of their induction is key to regulating pathogenesis. The importance of infection order is also seen in virus/bacterium coinfection systems. Bacterial infections secondary to IAV infection have been widely shown to have worse disease outcomes than either IAV or the bacterial infection alone (7, 56, 57). However, when these same bacterial pathogens are given to mice prior to IAV, they can reduce the severity of IAV (56, 58). This protective effect has been seen when *Streptococcus pneumoniae* was given to mice 10 days prior to PR8 and was associated with reduced inflammation in the lung without impacting viral loads. Bacterial pneumolysin was shown to be required for protection

by preventing IAV-mediated depletion of alveolar macrophages (56). Similarly, infection of mice with *Klebsiella pneumoniae* prior to PR8 protects against morbidity and mortality, which is associated with both reduced inflammation and viral load in the lungs of coinfected mice (58). In this coinfection system, *K. pneumoniae* was shown to reduce PR8-induced NK cell responses, which are known to promote disease pathology during PR8 infection (53, 58). Thus, the order of coinfecting pathogens is a critical determinant in disease outcomes across pathogen types and experimental systems. This is likely a reflection of the dual nature of innate immune responses: they stimulate effective immunity early in infection but contribute to immune-mediated pathology later in infection.

Interestingly, infection by MHV 2 days prior to PR8 also reduced the severity of PR8 infection. Unlike RV, MHV causes morbidity and mortality in mice, though virulence depends on the mouse strain (30, 31, 59). We have observed dose-dependent severity of MHV in BALB/c mice. Intranasal inoculation of 2×10^3 PFU resulted in clinical disease with low mortality (Fig. 7), while a dose of 2×10^5 caused 100% mortality (data not shown). However, reducing the dose of MHV to lessen disease resulted in less efficient protection upon coinfection with PR8. Thus, in order to achieve sufficient induction of a protective response, MHV-mediated disease was unavoidable. Interestingly, mice coinfected by MHV and PR8 had weight loss kinetics that closely mimicked MHV infection alone. We further observed that coinfected mice had lower PR8 loads in the lungs on day 2 than Mock/PR8-infected mice (Fig. 8), suggesting that disease early in coinfected mice was likely caused by MHV. In contrast, PR8 levels by day 4 were equivalent in Mock/PR8- and MHV/PR8-infected groups despite the significant protection of MHV/PR8-coinfected mice from mortality. The change in PR8 titers in the lungs was inversely correlated with IFN-β levels. This result is similar to a study that used poly(I·C) to protect aged mice from a lethal PR8 infection in which protected mice had strong induction of IFN-β and lower PR8 titers on day 2 but equivalent levels on day 4 (60). Future studies are needed to determine the role of this early type I IFN response in inducing later recovery from PR8 infection. Survival of BALB/c mice upon MHV-1 infection is dependent upon a type I IFN response (61). Furthermore, mouse strain-dependent resistance to MHV-1 disease corresponds with robust expression of type I IFNs (30). On the basis of these studies, we expect that the type I IFN response is adequate to protect BALB/c mice from a lower dose, but not a lethal dose, of MHV. Other components of the BALB/c immune response to MHV-1 infection have not been studied in detail. A complete understanding of this response will be important in determining the similarities and differences in the mechanisms whereby MHV and RV reduce the severity of PR8.

On the basis of our observations that either RV or MHV given 2 days before influenza A virus PR8 was effective at reducing the severity of PR8, we propose that these unrelated viruses are stimulating innate immune defenses that prime the response against PR8. Although both RV and MHV induced earlier IFN-β expression in coinfected mice than infection by PR8 alone, this response was associated with lower PR8 titers only in MHV/PR8-coinfected mice. This may be due to higher level of IFN-β expression in MHV/PR8-coinfected mice than in RV/PR8-coinfected mice. Furthermore, IFN-β expression was lower in coinfected mice than in Mock/PR8-infected mice by day 4 when viral loads remained high, suggesting that IFN-independent mechanisms contribute to reducing severity in coinfected mice. Several studies have evaluated stimulation of innate immunity in providing protection against influenza virus infections. As described above, bacterial pathogens given prior to influenza viruses can stimulate innate immunity that reduces the severity of influenza (56, 58). Infection of mice with nonpathogenic bacteria or with a parasite that causes a chronic infection has also been shown to reduce the severity of influenza infections (34, 62–65). While the mechanisms of protection may differ among coinfecting microbes, protection relies on detection of the initial infection by pattern recognition receptors. Stimulation of TLR signaling by agonists of TLR3 or TLR8 alone or TLR2/6 and TLR9 together provides significant protection against multiple influenza virus strains in mice (35, 60, 66, 67). Protection mediated by TLR2/6 and TLR9 activation is not associated with induction of a type I IFN response, suggesting that expression of proinflammatory cytokines and chemokines is

sufficient for protection (35). Furthermore, a dsRNA mimic protects mice from a number of IAV strains, and protection is at least partly independent of TLR3, which suggests that other dsRNA receptors, such as MDA5 and RIG-I may also promote protection (36). RV stimulates TLR3 and MDA5 to initiate type I and III interferon and inflammatory cytokine responses during infection (68–70). Stimulation of TLR2 in macrophages also contributes to the inflammatory response to RV1B infection in mice (71). MHV has mechanisms that prevent activation of IFN responses during viral replication in cells (72, 73); however, various TLRs contribute to protective responses in a cell type-dependent manner. TLR7 is required for MHV strain A59-induced type I IFN responses in plasmacytoid dendritic cells (74). Treatment of macrophages with a TLR3 agonist, but not a TLR2, TLR4, or TLR7 agonist, inhibits infection by multiple strains of MHV (75). TLR4 is the only pathogen recognition receptor that has been shown to contribute to protective responses against MHV-1 in mice (31). It will be important to determine the relative contributions of innate signaling pathways that lead to protective responses upon coinfection by RV or MHV.

Similar to our study, others have found that respiratory viruses can induce heterologous immunity, which is highly dependent upon the order and timing of viral inoculations. Infection of ferrets with the 2009 pandemic H1N1 influenza A virus (pdm09) 3 or 7 days before RSV prevented or reduced infection by RSV (76). In contrast, while RSV infection prior to pdm09 did not prevent infection or reduce virus shedding, it did reduce the severity of influenza disease. Although the mechanisms of protection in the ferret model have not been determined, pdm09 induces a stronger type I IFN response than RSV early in infection, which may inhibit coinfection by RSV (76). Although our viral inoculations were all within 2 days of each other, other studies have shown that infection of mice by one virus can alter the immune response to a heterologous virus given after resolution of the initial infection (77). Mice given lymphocytic choriomeningitis virus (LCMV), murine cytomegalovirus (MCMV), or PR8 6 weeks prior to vaccinia virus had reduced titers of vaccinia virus compared to those of control mice. However, infection with PR8 6 weeks prior to LCMV or MCMV increased titers of the second virus. Protection was associated with changing from a response dominated by neutrophils to lymphocytes or a Th2 response to a Th1 response. In contrast, when pigs were infected with porcine reproductive and respiratory syndrome virus, they had increased severity of porcine respiratory coronavirus infection, which corresponded with an increased Th1 cytokine response and reduced NK cell and type I IFN responses (78). Characterizing the immune responses across our various coinfection pairs and infection timings will provide insight into how different viruses mediate heterologous immunity and whether these mechanisms are generalizable.

MATERIALS AND METHODS

Virus stocks and cell lines. Madin-Darby canine kidney cells (MDCK) (ATCC CCL-34), murine fibroblast line 17Cl.1 (79) (provided by Kathryn Holmes, University of Colorado Denver School of Medicine), and HeLa cells (ATCC CCL-2) were grown in Dulbecco's modified Eagle medium (DMEM) supplemented with 10% fetal bovine serum (FBS; Atlanta Biologicals), and 1× antibiotic-antimycotic (ThermoFisher). Murine lung epithelial cells (LA-4) (ATCC CL-196) were grown in Ham's F12 (Kaign's modified) medium (F12K; Caisson) supplemented with 10% to 15% FBS and antibiotics. Influenza A virus PR8 (A/Puerto Rico/8/1934 [H1N1]), obtained from BEI Resources (NR-3169), was grown and titrated by 50% tissue culture infective dose ($TCID_{50}$) assay in MDCK cells. Mouse hepatitis virus MHV-1 (ATCC VR-261) was grown and titrated by plaque assay in 17Cl.1 cells. Rhinovirus RV1B (ATCC VR-1645) was grown and titrated by $TCID_{50}$ assay in HeLa cells. RV1B stocks were concentrated by centrifugation through 30% sucrose, and the virus pellet was resuspended in phosphate-buffered saline containing 2% FBS (PBS/2% FBS).

Mouse infections. All experimental protocols were approved by the University of Idaho Institutional Animal Care and Use Committee, following the *Guide for the Care and Use of Laboratory Animals* (80). As described below, mice were monitored daily and were euthanized by an overdose of sodium pentobarbital if they reached humane endpoints.

Six- to eight-week-old female BALB/c mice were purchased from Harlan Laboratories/Envigo. Mice were housed in individually vented cages with controlled light/dark cycles and regulated temperature maintained by University of Idaho Lab Animal Research Facilities and received food and water *ad libitum*. The mice were allowed to acclimatize to the facility for 5 to 12 days before experiments were performed under animal biosafety level 2 (ABSL2) conditions. Mice were anesthetized with inhaled isoflurane and

inoculated intranasally with 50 μl of virus. For coinfections, mice were inoculated with each virus 2 days apart or simultaneously in a total 50-μl volume. Control mice received mock inoculations of the same buffer or medium used for the respective virus: RV (PBS/2% FBS), PR8 (DMEM/1% bovine serum albumin [BSA]), or MHV (DMEM/10% FBS). See Results and figure legends for viral doses used in each experiment.

Mice were weighed and observed for clinical signs of disease daily and were humanely euthanized if they lost more than 25% of their starting weight or exhibited severe clinical signs of disease. Mice were given a daily severity score of 0 to 3 in each of four categories: ruffled fur, lethargy, labored breathing, and hunched posture. The daily scores were totaled for each individual mouse and averaged across the group of mice.

PR8 quantification. Right lobes of the lungs were flash-frozen and stored at −80°C. Frozen tissues were weighed and homogenized in DMEM with 2% BSA and 1% antibiotics, and PR8 was quantified by $TCID_{50}$ assay on MDCK cells (81). RV and MHV do not interfere with titration of PR8 in coinfected samples when the MDCK cell line is used (data not shown).

Quantitative RT-PCR. Lung tissue was stored in RNALater, and RNA was extracted using TRIzol (Invitrogen) or RNeasy Plus (Qiagen) according to the manufacturer's recommendations. One microgram of RNA was reverse transcribed using SuperScript IV VILO with ezDNase digestion (Invitrogen). Quantitative PCR was performed using PowerUp SYBR green and the StepOne Plus instrument (Applied Biosystems) using previously published IFN-β (82) and glyceraldehyde-3-phosphate dehydrogenase (GAPDH) (83) primer sets. Fold change compared to the values for mock-inoculated mice was calculated using the $2^{-\Delta\Delta Ct}$ method (84).

Histology and immunohistochemistry. The tracheas of euthanized mice were cannulated, and the lungs were inflated with 10% formalin before submerging the lungs in 10% formalin. After fixation, lungs were embedded in paraffin, cut in 5-μm sections, and stained with modified Harris hematoxylin and eosin (VWR Scientific). Lungs were processed for immunohistochemistry in the same manner as for histology. Tissue sections were deparaffinized, rehydrated, and subjected to heat-induced antigen retrieval in 10 mM sodium citrate buffer (pH 6) with 0.01% Tween 20. Endogenous peroxidase and alkaline phosphatase activities were inhibited with BLOXALL solution (Vector Laboratories). Lung sections were immunostained for the PR8 hemagglutinin (HA) protein using a polyclonal goat antibody (catalog no. NR-3148; BEI Resources) and an alkaline phosphatase-conjugated anti-goat antibody (ImmPRESS; Vector Laboratories) with detection by ImmPACT Vector red (Vector Laboratories) and counterstaining with hematoxylin. Images were acquired with a Zeiss Axio Lab.A1 microscope with an Axiocam 105 color camera using ZEN 2.3 software (Zeiss). Histopathology was analyzed in a blind manner by a pathologist. Serial images were acquired from two sections each from two mice per group, and inflamed areas of tissues were measured using ImageJ software (NIH). Estimated percentages of inflamed areas were calculated by the ratio of inflamed area over total tissue area analyzed. The percentages were averaged from the four replicate sections per group. Immunohistochemical staining was evaluated in a blind manner by a researcher to estimate the presence of viral antigen in bronchiolar epithelium, alveolar epithelium, and leukocytes, using one section each from two animals per group.

***In vitro* coinfection experiments.** LA-4 cells were inoculated with PR8 (multiplicity of infection [MOI] of 1) either 6 or 12 h after or simultaneously with inoculation with RV (MOI of 1). After 1 h of incubation with the inoculum, cells were washed twice with serum-free medium and then incubated in Ham's F12K medium with 2% FBS and antibiotics at 37°C. Supernatant medium was collected from the cells at 6, 12, 18, 24, 48, 72, and 96 h after PR8 inoculation, and PR8 was titrated by $TCID_{50}$ assay using MDCK cells.

Statistics. Statistical analyses were performed using Graphpad Prism 7 software. Survival curves were compared using log rank Mantel-Cox curve comparison. Weight loss and clinical score data were compared using multiple Student's *t* tests with Holm-Sidak multiple-comparison correction. PR8 titers from mouse lungs and cell culture experiments were compared using Student's *t* tests without correction for multiple comparisons.

ACKNOWLEDGMENTS

Research reported in this publication was supported by the National Institute of General Medical Sciences of the National Institutes of Health under award P20GM104420.

The content is solely the responsibility of the authors and does not necessarily represent the official views of the National Institutes of Health.

The following reagents were obtained through the NIH Biodefense and Emerging Infections Research Resources Repository, NIAID, NIH: influenza A virus A/Puerto Rico/8/34 (H1N1) and polyclonal anti-influenza virus H1 (H0) hemagglutinin (HA), A/Puerto Rico/8/34 (H1N1) antiserum, goat (NR-3148). We thank John Clary, Bhim Thapa, Jade Rodgers, and Alicia Healey for excellent technical support. We are also grateful to George Hodges for critically reviewing the pathology and manuscript.

REFERENCES

1. Brunstein JD, Cline CL, McKinney S, Thomas E. 2008. Evidence from multiplex molecular assays for complex multipathogen interactions in acute respiratory infections. J Clin Microbiol 46:97–102. https://doi.org/10.1128/JCM.01117-07.

2. Fairchok MP, Martin ET, Chambers S, Kuypers J, Behrens M, Braun LE, Englund JA. 2010. Epidemiology of viral respiratory tract infections in a prospective cohort of infants and toddlers attending daycare. J Clin Virol 49:16–20. https://doi.org/10.1016/j.jcv.2010.06.013.
3. Calvo C, García-García ML, Blanco C, Vázquez MC, Frías ME, Pérez-Breña P, Casas I. 2008. Multiple simultaneous viral infections in infants with acute respiratory tract infections in Spain. J Clin Virol 42:268–272. https://doi.org/10.1016/j.jcv.2008.03.012.
4. Nolan VG, Arnold SR, Bramley AM, Ampofo K, Williams DJ, Grijalva CG, Self WH, Anderson EJ, Wunderink RG, Edwards KM, Pavia AT, Jain S, McCullers JA. 2018. Etiology and impact of coinfections in children hospitalized with community-acquired pneumonia. J Infect Dis 218:179–188. https://doi.org/10.1093/infdis/jix641.
5. DaPalma T, Doonan BP, Trager NM, Kasman LM. 2010. A systematic approach to virus-virus interactions. Virus Res 149:1–9. https://doi.org/10.1016/j.virusres.2010.01.002.
6. Opatowski L, Baguelin M, Eggo RM. 2018. Influenza interaction with cocirculating pathogens and its impact on surveillance, pathogenesis, and epidemic profile: a key role for mathematical modelling. PLoS Pathog 14:e1006770. https://doi.org/10.1371/journal.ppat.1006770.
7. Robinson KM, Kolls JK, Alcorn JF. 2015. The immunology of influenza virus-associated bacterial pneumonia. Curr Opin Immunol 34:59–67. https://doi.org/10.1016/j.coi.2015.02.002.
8. Jain S, Williams DJ, Arnold SR, Ampofo K, Bramley AM, Reed C, Stockmann C, Anderson EJ, Grijalva CG, Self WH, Zhu Y, Patel A, Hymas W, Chappell JD, Kaufman RA, Kan JH, Dansie D, Lenny N, Hillyard DR, Haynes LM, Levine M, Lindstrom S, Winchell JM, Katz JM, Erdman D, Schneider E, Hicks LA, Wunderink RG, Edwards KM, Pavia AT, McCullers JA, Finelli L, CDC EPIC Study Team. 2015. Community-acquired pneumonia requiring hospitalization among U.S. children. N Engl J Med 372:835–845. https://doi.org/10.1056/NEJMoa1405870.
9. Grondahl B, Ankermann T, von Bismarck P, Rockahr S, Kowalzik F, Gehring S, Meyer C, Knuf M, Puppe W. 2014. The 2009 pandemic influenza A(H1N1) coincides with changes in the epidemiology of other viral pathogens causing acute respiratory tract infections in children. Infection 42:303–308. https://doi.org/10.1007/s15010-013-0545-5.
10. Greer RM, McErlean P, Arden KE, Faux CE, Nitsche A, Lambert SB, Nissen MD, Sloots TP, Mackay IM. 2009. Do rhinoviruses reduce the probability of viral co-detection during acute respiratory tract infections? J Clin Virol 45:10–15. https://doi.org/10.1016/j.jcv.2009.03.008.
11. Esper FP, Spahlinger T, Zhou L. 2011. Rate and influence of respiratory virus co-infection on pandemic (H1N1) influenza disease. J Infect 63:260–266. https://doi.org/10.1016/j.jinf.2011.04.004.
12. Papadopoulos NG, Moustaki M, Tsolia M, Bossios A, Astra E, Prezerakou A, Gourgiotis D, Kafetzis D. 2002. Association of rhinovirus infection with increased disease severity in acute bronchiolitis. Am J Respir Crit Care Med 165:1285–1289. https://doi.org/10.1164/rccm.200112-118BC.
13. Aberle JH, Aberle SW, Pracher E, Hutter HP, Kundi M, Popow-Kraupp T. 2005. Single versus dual respiratory virus infections in hospitalized infants: impact on clinical course of disease and interferon-gamma response. Pediatr Infect Dis J 24:605–610. https://doi.org/10.1097/01.inf.0000168741.59747.2d.
14. Marcos MA, Ramon S, Anton A, Martinez E, Vilella A, Olive V, Cilloniz C, Moreno A, Torres A, Pumarola T. 2011. Clinical relevance of mixed respiratory viral infections in adults with influenza A H1N1. Eur Respir J 38:739–742. https://doi.org/10.1183/09031936.00168610.
15. Martin ET, Kuypers J, Wald A, Englund JA. 2012. Multiple versus single virus respiratory infections: viral load and clinical disease severity in hospitalized children. Influenza Other Respir Viruses 6:71–77. https://doi.org/10.1111/j.1750-2659.2011.00265.x.
16. Martínez-Roig A, Salvadó M, Caballero-Rabasco MA, Sánchez-Buenavida A, López-Segura N, Bonet-Alcaina M. 2015. Viral coinfection in childhood respiratory tract infections. Arch Bronconeumol 51:5–9. https://doi.org/10.1016/j.arbres.2014.01.018.
17. Camargo C, Guatura SB, Bellei N. 2012. Respiratory viral coinfection among hospitalized patients with H1N1 2009 during the first pandemic wave in Brazil. Braz J Infect Dis 16:180–183.
18. Yoshida LM, Suzuki M, Nguyen HA, Le MN, Dinh Vu T, Yoshino H, Schmidt WP, Nguyen TT, Le HT, Morimoto K, Moriuchi H, Dang DA, Ariyoshi K. 2013. Respiratory syncytial virus: co-infection and paediatric lower respiratory tract infections. Eur Respir J 42:461–469. https://doi.org/10.1183/09031936.00101812.
19. Marguet C, Lubrano M, Gueudin M, Le Roux P, Deschildre A, Forget C, Couderc L, Siret D, Donnou MD, Bubenheim M, Vabret A, Freymuth F. 2009. In very young infants severity of acute bronchiolitis depends on carried viruses. PLoS One 4:e4596. https://doi.org/10.1371/journal.pone.0004596.
20. Richard N, Komurian-Pradel F, Javouhey E, Perret M, Rajoharison A, Bagnaud A, Billaud G, Vernet G, Lina B, Floret D, Paranhos-Baccalà G. 2008. The impact of dual viral infection in infants admitted to a pediatric intensive care unit associated with severe bronchiolitis. Pediatr Infect Dis J 27:213–217. https://doi.org/10.1097/INF.0b013e31815b4935.
21. Anestad G, Nordbo SA. 2011. Virus interference. Did rhinoviruses activity hamper the progress of the 2009 influenza A (H1N1) pandemic in Norway? Med Hypotheses 77:1132–1134. https://doi.org/10.1016/j.mehy.2011.09.021.
22. Casalegno JS, Ottmann M, Duchamp MB, Escuret V, Billaud G, Frobert E, Morfin F, Lina B. 2010. Rhinoviruses delayed the circulation of the pandemic influenza A (H1N1) 2009 virus in France. Clin Microbiol Infect 16:326–329. https://doi.org/10.1111/j.1469-0691.2010.03167.x.
23. Linde A, Rotzén-Östlund M, Zweygberg-Wirgart B, Rubinova S, Brytting M. 2009. Does viral interference affect spread of influenza? Euro Surveill 14(40):pii=19354.
24. Pascalis H, Temmam S, Turpin M, Rollot O, Flahault A, Carrat F, de Lamballerie X, Gerardin P, Dellagi K. 2012. Intense co-circulation of non-influenza respiratory viruses during the first wave of pandemic influenza pH1N1/2009: a cohort study in Reunion Island. PLoS One 7:e44755. https://doi.org/10.1371/journal.pone.0044755.
25. Vogel AJ, Harris S, Marsteller N, Condon SA, Brown DM. 2014. Early cytokine dysregulation and viral replication are associated with mortality during lethal influenza infection. Viral Immunol 27:214–224. https://doi.org/10.1089/vim.2013.0095.
26. Fukushi M, Ito T, Oka T, Kitazawa T, Miyoshi-Akiyama T, Kirikae T, Yamashita M, Kudo K. 2011. Serial histopathological examination of the lungs of mice infected with influenza A virus PR8 strain. PLoS One 6:e21207. https://doi.org/10.1371/journal.pone.0021207.
27. Sugamata R, Dobashi H, Nagao T, Yamamoto K, Nakajima N, Sato Y, Aratani Y, Oshima M, Sata T, Kobayashi K, Kawachi S, Nakayama T, Suzuki K. 2012. Contribution of neutrophil-derived myeloperoxidase in the early phase of fulminant acute respiratory distress syndrome induced by influenza virus infection. Microbiol Immunol 56:171–182. https://doi.org/10.1111/j.1348-0421.2011.00424.x.
28. Tuthill TJ, Papadopoulos NG, Jourdan P, Challinor LJ, Sharp NA, Plumpton C, Shah K, Barnard S, Dash L, Burnet J, Killington RA, Rowlands DJ, Clarke NJ, Blair ED, Johnston SL. 2003. Mouse respiratory epithelial cells support efficient replication of human rhinovirus. J Gen Virol 84:2829–2836. https://doi.org/10.1099/vir.0.19109-0.
29. Bartlett NW, Walton RP, Edwards MR, Aniscenko J, Caramori G, Zhu J, Glanville N, Choy KJ, Jourdan P, Burnet J, Tuthill TJ, Pedrick MS, Hurle MJ, Plumpton C, Sharp NA, Bussell JN, Swallow DM, Schwarze J, Guy B, Almond JW, Jeffery PK, Lloyd CM, Papi A, Killington RA, Rowlands DJ, Blair ED, Clarke NJ, Johnston SL. 2008. Mouse models of rhinovirus-induced disease and exacerbation of allergic airway inflammation. Nat Med 14:199–204. https://doi.org/10.1038/nm1713.
30. De Albuquerque N, Baig E, Ma X, Zhang J, He W, Rowe A, Habal M, Liu M, Shalev I, Downey GP, Gorczynski R, Butany J, Leibowitz J, Weiss SR, McGilvray ID, Phillips MJ, Fish EN, Levy GA. 2006. Murine hepatitis virus strain 1 produces a clinically relevant model of severe acute respiratory syndrome in A/J mice. J Virol 80:10382–10394. https://doi.org/10.1128/JVI.00747-06.
31. Khanolkar A, Hartwig SM, Haag BA, Meyerholz DK, Harty JT, Varga SM. 2009. Toll-like receptor 4 deficiency increases disease and mortality after mouse hepatitis virus type 1 infection of susceptible C3H mice. J Virol 83:8946–8956. https://doi.org/10.1128/JVI.01857-08.
32. Gonzalez AJ, Ijezie EC, Balemba OB, Miura TA. 2018. Attenuation of influenza A virus disease severity by viral co-infection in a mouse model. bioRxiv https://doi.org/10.1101/326546.
33. VanLeuven JT, Ridenhour BJ, Gonzalez AJ, Miller CR, Miura TA. 2017. Lung epithelial cells have virus-specific and shared gene expression responses to infection by diverse respiratory viruses. PLoS One 12:e0178408. https://doi.org/10.1371/journal.pone.0178408.
34. Li R, Lim A, Phoon MC, Narasaraju T, Ng JK, Poh WP, Sim MK, Chow VT, Locht C, Alonso S. 2010. Attenuated *Bordetella pertussis* protects against highly pathogenic influenza A viruses by dampening the cytokine storm. J Virol 84:7105–7113. https://doi.org/10.1128/JVI.02542-09.
35. Tuvim MJ, Gilbert BE, Dickey BF, Evans SE. 2012. Synergistic TLR2/6 and TLR9 activation protects mice against lethal influenza pneumonia. PLoS One 7:e30596. https://doi.org/10.1371/journal.pone.0030596.

36. Lau YF, Tang LH, Ooi EE, Subbarao K. 2010. Activation of the innate immune system provides broad-spectrum protection against influenza A viruses with pandemic potential in mice. Virology 406:80–87. https://doi.org/10.1016/j.virol.2010.07.008.
37. Shinjoh M, Omoe K, Saito N, Matsuo N, Nerome K. 2000. In vitro growth profiles of respiratory syncytial virus in the presence of influenza virus. Acta Virol 44:91–97.
38. Goto H, Ihira H, Morishita K, Tsuchiya M, Ohta K, Yumine N, Tsurudome M, Nishio M. 2016. Enhanced growth of influenza A virus by coinfection with human parainfluenza virus type 2. Med Microbiol Immunol 205:209–218. https://doi.org/10.1007/s00430-015-0441-y.
39. Garcia-Sastre A, Egorov A, Matassov D, Brandt S, Levy DE, Durbin JE, Palese P, Muster T. 1998. Influenza A virus lacking the NS1 gene replicates in interferon-deficient systems. Virology 252:324–330. https://doi.org/10.1006/viro.1998.9508.
40. Glanville N, Peel TJ, Schroder A, Aniscenko J, Walton RP, Finotto S, Johnston SL. 2016. Tbet deficiency causes T helper cell dependent airways eosinophilia and mucus hypersecretion in response to rhinovirus infection. PLoS Pathog 12:e1005913. https://doi.org/10.1371/journal.ppat.1005913.
41. Girkin J, Hatchwell L, Foster P, Johnston SL, Bartlett N, Collison A, Mattes J. 2015. CCL7 and IRF-7 mediate hallmark inflammatory and IFN responses following rhinovirus 1B infection. J Immunol 194:4924–4930. https://doi.org/10.4049/jimmunol.1401362.
42. Seo SU, Kwon HJ, Ko HJ, Byun YH, Seong BL, Uematsu S, Akira S, Kweon MN. 2011. Type I interferon signaling regulates Ly6C(hi) monocytes and neutrophils during acute viral pneumonia in mice. PLoS Pathog 7:e1001304. https://doi.org/10.1371/journal.ppat.1001304.
43. Stifter SA, Bhattacharyya N, Pillay R, Florido M, Triccas JA, Britton WJ, Feng CG. 2016. Functional interplay between type I and II interferons is essential to limit influenza A virus-induced tissue inflammation. PLoS Pathog 12:e1005378. https://doi.org/10.1371/journal.ppat.1005378.
44. Chung Y, Hong JY, Lei J, Chen Q, Bentley JK, Hershenson MB. 2015. Rhinovirus infection induces interleukin-13 production from CD11b-positive, M2-polarized exudative macrophages. Am J Respir Cell Mol Biol 52:205–216. https://doi.org/10.1165/rcmb.2014-0068OC.
45. Ganesan S, Pham D, Jing Y, Farazuddin M, Hudy MH, Unger B, Comstock AT, Proud D, Lauring AS, Sajjan US. 2016. TLR2 activation limits rhinovirus-stimulated CXCL-10 by attenuating IRAK-1-dependent IL-33 receptor signaling in human bronchial epithelial cells. J Immunol 197:2409–2420. https://doi.org/10.4049/jimmunol.1502702.
46. Oshansky CM, Gartland AJ, Wong SS, Jeevan T, Wang D, Roddam PL, Caniza MA, Hertz T, Devincenzo JP, Webby RJ, Thomas PG. 2014. Mucosal immune responses predict clinical outcomes during influenza infection independently of age and viral load. Am J Respir Crit Care Med 189:449–462. https://doi.org/10.1164/rccm.201309-1616OC.
47. Rutigliano JA, Sharma S, Morris MY, Oguin TH, III, McClaren JL, Doherty PC, Thomas PG. 2014. Highly pathological influenza A virus infection is associated with augmented expression of PD-1 by functionally compromised virus-specific CD8+ T cells. J Virol 88:1636–1651. https://doi.org/10.1128/JVI.02851-13.
48. Lin KL, Suzuki Y, Nakano H, Ramsburg E, Gunn MD. 2008. CCR2+ monocyte-derived dendritic cells and exudate macrophages produce influenza-induced pulmonary immune pathology and mortality. J Immunol 180:2562–2572. https://doi.org/10.4049/jimmunol.180.4.2562.
49. Le Goffic R, Balloy V, Lagranderie M, Alexopoulou L, Escriou N, Flavell R, Chignard M, Si-Tahar M. 2006. Detrimental contribution of the Toll-like receptor (TLR)3 to influenza A virus-induced acute pneumonia. PLoS Pathog 2:e53. https://doi.org/10.1371/journal.ppat.0020053.
50. Unger BL, Faris AN, Ganesan S, Comstock AT, Hershenson MB, Sajjan US. 2012. Rhinovirus attenuates non-typeable *Hemophilus influenzae*-stimulated IL-8 responses via TLR2-dependent degradation of IRAK-1. PLoS Pathog 8:e1002969. https://doi.org/10.1371/journal.ppat.1002969.
51. Narasaraju T, Yang E, Samy RP, Ng HH, Poh WP, Liew AA, Phoon MC, van Rooijen N, Chow VT. 2011. Excessive neutrophils and neutrophil extracellular traps contribute to acute lung injury of influenza pneumonitis. Am J Pathol 179:199–210. https://doi.org/10.1016/j.ajpath.2011.03.013.
52. Ichikawa A, Kuba K, Morita M, Chida S, Tezuka H, Hara H, Sasaki T, Ohteki T, Ranieri VM, dos Santos CC, Kawaoka Y, Akira S, Luster AD, Lu B, Penninger JM, Uhlig S, Slutsky AS, Imai Y. 2013. CXCL10-CXCR3 enhances the development of neutrophil-mediated fulminant lung injury of viral and nonviral origin. Am J Respir Crit Care Med 187:65–77. https://doi.org/10.1164/rccm.201203-0508OC.
53. Zhou G, Juang SW, Kane KP. 2013. NK cells exacerbate the pathology of influenza virus infection in mice. Eur J Immunol 43:929–938. https://doi.org/10.1002/eji.201242620.
54. Marois I, Cloutier A, Garneau E, Richter MV. 2012. Initial infectious dose dictates the innate, adaptive, and memory responses to influenza in the respiratory tract. J Leukoc Biol 92:107–121. https://doi.org/10.1189/jlb.1011490.
55. Davidson S, Crotta S, McCabe TM, Wack A. 2014. Pathogenic potential of interferon alphabeta in acute influenza infection. Nat Commun 5:3864. https://doi.org/10.1038/ncomms4864.
56. Wolf AI, Strauman MC, Mozdzanowska K, Williams KL, Osborne LC, Shen H, Liu Q, Garlick D, Artis D, Hensley SE, Caton AJ, Weiser JN, Erikson J. 2014. Pneumolysin expression by *Streptococcus pneumoniae* protects colonized mice from influenza virus-induced disease. Virology 462-463:254–265. https://doi.org/10.1016/j.virol.2014.06.019.
57. Haynes L, Szaba FM, Eaton SM, Kummer LW, Lanthier PA, Petell AH, Duso DK, Luo D, Lin JS, Lefebvre JS, Randall TD, Johnson LL, Kohlmeier JE, Woodland DL, Smiley ST. 2012. Immunity to the conserved influenza nucleoprotein reduces susceptibility to secondary bacterial infections. J Immunol 189:4921–4929. https://doi.org/10.4049/jimmunol.1201916.
58. Wang J, Li F, Sun R, Gao X, Wei H, Tian Z. 2014. *Klebsiella pneumoniae* alleviates influenza-induced acute lung injury via limiting NK cell expansion. J Immunol 193:1133–1141. https://doi.org/10.4049/jimmunol.1303303.
59. Khanolkar A, Hartwig SM, Haag BA, Meyerholz DK, Epping LL, Haring JS, Varga SM, Harty JT. 2009. Protective and pathologic roles of the immune response to mouse hepatitis virus type 1: implications for severe acute respiratory syndrome. J Virol 83:9258–9272. https://doi.org/10.1128/JVI.00355-09.
60. Zhao J, Wohlford-Lenane C, Zhao J, Fleming E, Lane TE, McCray PB, Jr, Perlman S. 2012. Intranasal treatment with poly(I·C) protects aged mice from lethal respiratory virus infections. J Virol 86:11416–11424. https://doi.org/10.1128/JVI.01410-12.
61. Channappanavar R, Fehr AR, Vijay R, Mack M, Zhao J, Meyerholz DK, Perlman S. 2016. Dysregulated type I interferon and inflammatory monocyte-macrophage responses cause lethal pneumonia in SARS-CoV-infected mice. Cell Host Microbe 19:181–193. https://doi.org/10.1016/j.chom.2016.01.007.
62. Kamble NM, Hajam IA, Lee JH. 2017. Orally administered live attenuated *Salmonella typhimurium* protects mice against lethal infection with H1N1 influenza virus. Vet Microbiol 201:1–6. https://doi.org/10.1016/j.vetmic.2017.01.006.
63. Park MK, Ngo V, Kwon YM, Lee YT, Yoo S, Cho YH, Hong SM, Hwang HS, Ko EJ, Jung YJ, Moon DW, Jeong EJ, Kim MC, Lee YN, Jang JH, Oh JS, Kim CH, Kang SM. 2013. *Lactobacillus plantarum* DK119 as a probiotic confers protection against influenza virus by modulating innate immunity. PLoS One 8:e75368. https://doi.org/10.1371/journal.pone.0075368.
64. Jung YJ, Lee YT, Ngo VL, Cho YH, Ko EJ, Hong SM, Kim KH, Jang JH, Oh JS, Park MK, Kim CH, Sun J, Kang SM. 2017. Heat-killed *Lactobacillus casei* confers broad protection against influenza A virus primary infection and develops heterosubtypic immunity against future secondary infection. Sci Rep 7:17360. https://doi.org/10.1038/s41598-017-17487-8.
65. Scheer S, Krempl C, Kallfass C, Frey S, Jakob T, Mouahid G, Mone H, Schmitt-Graff A, Staeheli P, Lamers MC. 2014. *S. mansoni* bolsters antiviral immunity in the murine respiratory tract. PLoS One 9:e112469. https://doi.org/10.1371/journal.pone.0112469.
66. Leiva-Juarez MM, Kirkpatrick CT, Gilbert BE, Scott B, Tuvim MJ, Dickey BF, Evans SE, Markesich D. 2018. Combined aerosolized Toll-like receptor ligands are an effective therapeutic agent against influenza pneumonia when co-administered with oseltamivir. Eur J Pharmacol 818:191–197. https://doi.org/10.1016/j.ejphar.2017.10.035.
67. Wong JP, Christopher ME, Viswanathan S, Karpoff N, Dai X, Das D, Sun LQ, Wang M, Salazar AM. 2009. Activation of toll-like receptor signaling pathway for protection against influenza virus infection. Vaccine 27:3481–3483. https://doi.org/10.1016/j.vaccine.2009.01.048.
68. Slater L, Bartlett NW, Haas JJ, Zhu J, Message SD, Walton RP, Sykes A, Dahdaleh S, Clarke DL, Belvisi MG, Kon OM, Fujita T, Jeffery PK, Johnston SL, Edwards MR. 2010. Co-ordinated role of TLR3, RIG-I and MDA5 in the innate response to rhinovirus in bronchial epithelium. PLoS Pathog 6:e1001178. https://doi.org/10.1371/journal.ppat.1001178.
69. Wang Q, Nagarkar DR, Bowman ER, Schneider D, Gosangi B, Lei J, Zhao Y, McHenry CL, Burgens RV, Miller DJ, Sajjan U, Hershenson MB. 2009. Role of double-stranded RNA pattern recognition receptors in rhinovirus-induced airway epithelial cell responses. J Immunol 183:6989–6997. https://doi.org/10.4049/jimmunol.0901386.

70. Wang Q, Miller DJ, Bowman ER, Nagarkar DR, Schneider D, Zhao Y, Linn MJ, Goldsmith AM, Bentley JK, Sajjan US, Hershenson MB. 2011. MDA5 and TLR3 initiate pro-inflammatory signaling pathways leading to rhinovirus-induced airways inflammation and hyperresponsiveness. PLoS Pathog 7:e1002070. https://doi.org/10.1371/journal.ppat.1002070.
71. Han M, Chung Y, Young Hong J, Rajput C, Lei J, Hinde JL, Chen Q, Weng SP, Bentley JK, Hershenson MB. 2016. Toll-like receptor 2-expressing macrophages are required and sufficient for rhinovirus-induced airway inflammation. J Allergy Clin Immunol 138:1619–1630. https://doi.org/10.1016/j.jaci.2016.01.037.
72. Deng X, Hackbart M, Mettelman RC, O'Brien A, Mielech AM, Yi G, Kao CC, Baker SC. 2017. Coronavirus nonstructural protein 15 mediates evasion of dsRNA sensors and limits apoptosis in macrophages. Proc Natl Acad Sci U S A 114:E4251–E4260. https://doi.org/10.1073/pnas.1618310114.
73. Kindler E, Gil-Cruz C, Spanier J, Li Y, Wilhelm J, Rabouw HH, Züst R, Hwang M, V'kovski P, Stalder H, Marti S, Habjan M, Cervantes-Barragan L, Elliot R, Karl N, Gaughan C, van Kuppeveld FJM, Silverman RH, Keller M, Ludewig B, Bergmann CC, Ziebuhr J, Weiss SR, Kalinke U, Thiel V. 2017. Early endonuclease-mediated evasion of RNA sensing ensures efficient coronavirus replication. PLoS Pathog 13:e1006195. https://doi.org/10.1371/journal.ppat.1006195.
74. Cervantes-Barragan L, Zust R, Weber F, Spiegel M, Lang KS, Akira S, Thiel V, Ludewig B. 2007. Control of coronavirus infection through plasmacytoid dendritic-cell-derived type I interferon. Blood 109:1131–1137. https://doi.org/10.1182/blood-2006-05-023770.
75. Mazaleuskaya L, Veltrop R, Ikpeze N, Martin-Garcia J, Navas-Martin S. 2012. Protective role of Toll-like receptor 3-induced type I interferon in murine coronavirus infection of macrophages. Viruses 4:901–923. https://doi.org/10.3390/v4050901.
76. Chan KF, Carolan LA, Korenkov D, Druce J, McCaw J, Reading PC, Barr IG, Laurie KL. 2018. Investigating viral interference between influenza A virus and human respiratory syncytial virus in a ferret model of infection. J Infect Dis 218:406–417. https://doi.org/10.1093/infdis/jiy184.
77. Chen HD, Fraire AE, Joris I, Welsh RM, Selin LK. 2003. Specific history of heterologous virus infections determines anti-viral immunity and immunopathology in the lung. Am J Pathol 163:1341–1355. https://doi.org/10.1016/S0002-9440(10)63493-1.
78. Jung K, Renukaradhya GJ, Alekseev KP, Fang Y, Tang Y, Saif LJ. 2009. Porcine reproductive and respiratory syndrome virus modifies innate immunity and alters disease outcome in pigs subsequently infected with porcine respiratory coronavirus: implications for respiratory viral co-infections. J Gen Virol 90:2713–2723. https://doi.org/10.1099/vir.0.014001-0.
79. Sturman LS, Takemoto KK. 1972. Enhanced growth of a murine coronavirus in transformed mouse cells. Infect Immun 6:501–507.
80. National Research Council. 2011. Guide for the care and use of laboratory animals, 8th ed. National Academies PressWashington, DC.
81. Szretter KJ, Balish AL, Katz JM. 2006. Influenza: propagation, quantification, and storage. Curr Protoc Microbiol Chapter 15:Unit 15G.1.
82. Sommereyns C, Paul S, Staeheli P, Michiels T. 2008. IFN-lambda (IFN-lambda) is expressed in a tissue-dependent fashion and primarily acts on epithelial cells in vivo. PLoS Pathog 4:e1000017. https://doi.org/10.1371/journal.ppat.1000017.
83. Jones PH, Mehta HV, Maric M, Roller RJ, Okeoma CM. 2012. Bone marrow stromal cell antigen 2 (BST-2) restricts mouse mammary tumor virus (MMTV) replication in vivo. Retrovirology 9:10. https://doi.org/10.1186/1742-4690-9-10.
84. Livak KJ, Schmittgen TD. 2001. Analysis of relative gene expression data using real-time quantitative PCR and the 2(-Delta Delta C(T)) method. Methods 25:402–408. https://doi.org/10.1006/meth.2001.1262.